Magnitude of latent heat in thermally loaded clays

Sergio Samat, Laurent Brochard, Ioannis Stefanou

Received: Added at production | Revised: Added at production | Accepted: Added at production

DOI: xxx/xxxx

ARTICLE TYPE

Magnitude of latent heat in thermally loaded clays

Sergio SAMAT[1] | Laurent BROCHARD[1] | Ioannis STEFANOU[2]

[1]Laboratoire Navier, ENPC, Paris, France
[2]Civil engineering, ECN, Nantes, France

Correspondence
*Sergio SAMAT, Email: sergio-luis.samat@enpc.fr

Present Address
Laboratoire Navier, ENPC, 6-8 Avenue Blaise Pascal, 77420 Champs-sur-Marne. Paris, France.

Abstract

Temperature changes are known to induce specific couplings in clay, in particular, an anomalously high thermal pressurization in undrained conditions, or a thermal compaction in drained conditions, both of which are potential threats for the mechanical stability and sealing capacity of the geomaterials. Thermodynamical analysis of those peculiar thermo-mechanical couplings points to a potentially important latent energy which in turn could limit the temperature change upon heating or cooling. The direct measurement of latent energy developed during a laboratory geomechanical test is challenging. Instead, proper identification of thermal hardening in conventional experiments with temperature changes provides an alternative route to estimate latent energy. In this work, existing laboratory thermomechanical tests of clays are analyzed with a rigorous thermodynamic framework to quantify the magnitude of latent energy in thermo-mechanically loaded clays. A thermodynamically consistent constitutive model for fully saturated clays that combines two key features: i) the temperature dependence of the blocked energy and ii) the framework of bounding plasticity, is proposed. The performance of the model is validated by reproducing results obtained in laboratory tests for Boom and Opalinus clays. The thermomechanical loads considered to validate the model performance, were then used to estimate the percentage of work that remains latent in the clayey material during plastic yielding. We find that the magnitude of latent energy is quite significant, typically a few tens of percent of the total dissipated energy, and increases significantly with temperature. Accordingly, it is expected to play an important role in the thermo-mechanical response of clays.

KEYWORDS:
Clays, Latent energy, Blocked energy, Thermal expansion, Thermal pressurization, Thermal hardening.

1 | INTRODUCTION

Nowadays, clayey materials are involved in several engineering applications. One of the active fields in which the thermal behavior of clays, and geomaterials in general, is important is that of deep geological storage and disposal of high-level nuclear waste (HLW). The main purpose of the geological disposal is to eliminate it from the human environment. The canisters that contain the HLW are placed down horizontally or vertically to a depth of hundreds of meters in the host rock. The space between the canister and the host rock is usually filled with a compacted swelling clay (bentonite) that acts as an additional engineering barrier to isolate the nuclear waste. The clay barrier is initially subjected to important pore pressurization, which is known to be usually high for water in clays when the flow conditions of the fluid filling the pore space are almost undrained (transient regime) due to the temperature rise that arises from the canister. This phenomenon occurs in clays when they are rapidly heated. It is due to the fact, that heat transfer is much faster than water flow and the thermal dilation coefficient of water is much larger than that of the solid phase[1,2,3]. Over long-times, when the flow conditions are almost drained (stationary regime) one faces another potential problem which is the unusual thermal compaction. Elevated temperatures induce a compactant irreversible deformation as long as the ratio between the mean yield stress of the material and the current in-situ mean effective stress is one, i.e. normal consolidation condition[4,5,2]. Temperature affects almost all the phenomena involved in the problem[1] consequently, proper geomechanical modeling has to pay special attention to the effects of temperature. Thermal behavior of clays is also important in the study and analysis of gouge faults. The reactivation of these faults due to tectonic displacements has effects that are often devastating. As a consequence, their analysis and possible mitigation are of interest for many geological surveys of the affected countries. Once a gouge fault is seismically reactivated significant irreversible shearing deformations develop, which cause high temperatures in the fault zone[6,7]. Pore pressure increase due to thermal effects is critical for the analysis of fault stability. This increase in pore pressure grows significantly in clay-rich faults. It has been proven that even when the clay fraction is relatively small, its influence in the global thermo-hydro-mechanical response is decisive[8]. Predicting consequences (e.g. possible leakages, instabilities risk) is of interest for those applications (e.g. ensuring confinement of nuclear wastes, forecast the response of a fault) requiring a deep understanding of the thermo-hydro-mechanical behavior of clays and proper knowledge of thermal pressurization since it is first-order in the stability of geomaterials.

All those applications involve coupled processes of fluid flow, heat transport, mass transport and deformation of the porous solid. The mathematical description of the balance equations that specify the coupled processes in the porous medium are recalled hereafter on the basis of considering it as an heterogeneous system, where the fluid and the porous solid interact between them. The balance equations and the constitutive laws are stated at the macroscopic level. In particular, in classical thermomechanical formulations the energy balance is expressed in terms of the rate of heat received by the material $\dot{Q}$ plus the mechanical dissipation d_s. As a consequence, all the mechanical work is dissipated in the form of heat. However, thermodynamic formulations for continuum[9], porous continuum[10] and experimental evidences[11] have shown that part of the rate of heat remains latent. As a consequence, an additional term emerges in the thermal balance, the *latent energy*. The latent energies transforming the states of stress[9] and hardening[10] have shown to be temperature-dependent and, it is for this reason that they are increasingly significant in the mentioned applications, where the temperature can be raised to high values (i.e. hundred of degree Celsius). Latent energy has been most often ignored in conventional thermo-mechanical formulations of soil mechanics. The reason might be that calorific energies that develop during elastoplastic processes are very weak and their reliable measurement is very difficult. As a consequence, calorimetric tests are rarely performed in geomechanical testing. As an example of calorimetric measurements carried out in mechanical tests, it is worth highlighting the work of Taylor and Quinney[12]. They performed calorimetric tests to measure the latent heat of plastic distortion in samples of rapidly twisted steel bars. Twisting the bars allowed to develop more plastic distortion in the bars than stretching them and consequently an increased accuracy in the measurements of energy

[0]**Nomenclature:** $\dot{Q}$, rate of heat; c_p, specific heat capacity of the porous medium; T, temperature; k_T, thermal conductivity; d_s, mechanical dissipation; e_f, internal energy of the fluid; s_f, specific entropy of the fluid; e_s, internal energy of the solid; s_s, specific entropy of the solid; ϕ, porosity; ε_{ij}, strain tensor; χ_{ij}, internal strain-like variable; ρ_f, fluid density; P, pore pressure; σ'_{ij}, effective stress tensor; ρ, dry density; δ_{ij}, Kronecker delta; f_s, Helmholtz free energy of the solid; g_f, Gibbs free enthalpy of the fluid; V, blocked energy; ε^p_{ij}, plastic strain tensor; m_f, wet density; ζ_{ij}, back stress tensor; x_{ij}, thermodynamic stress tensor; C_{th}, thermal diffusivity; L, latent energy; α_f, thermal expansion of the fluid; α, thermal expansion of the solid; α_p, plastic thermal contraction of the solid; G, shear modulus; κ^e, slope of isotropic compression line; M_c, slope of the critical state line; p_c, preconsolidation; f^y, yield surface; μ, chemical potential; K_f, bulk modulus of the fluid; c^p_f, volumetric heat capacity of the fluid; g_s, Gibbs energy of the solid; p', mean effective stress; q, deviatoric stress; ε^p_v, plastic volumetric strain; ε^p_s, plastic deviatoric strain; g_e, elastic Gibbs energy; K, bulk modulus; c^e_s, specific heat capacity at cte. stress; K^p, bulk modulus of material hardening; c^b_s, specific heat capacity associated to the blocked energy; L_χ, latent energy of hardening state transformation; κ^p, slope of the normal compression line; p^B_c, preconsolidation at bounding; f^B, bounding surface; $\bar{d}_s$, dissipation rate at bounding; p_x, thermodynamic mean stress; $\bar{p}_x$, image thermodynamic mean stress; $\bar{V}$, enhanced blocked energy; δ, radial distance; $\bar{g}_s$, scaled Gibbs energy; $\bar{p}'$, mean effective stress at bounding; H_p, plastic modulus of pure yielding; H_δ, bounding modulus

released as heat. The latent energy was then indirectly obtained as the difference between the measures of work done and released heat during plastic deformations.

The impact of latent energy in clays is difficult to predict, nevertheless important. While in other geomaterials this energy may be negligible, the micro-structural characteristics of clays formed by layers of minerals with adsorbed water make them highly sensitive to hydration and temperature [13,2]. In particular, saturated clays exhibit an anomalous response when they are thermally loaded. In drained conditions and initial states of over-consolidation, an increase of temperature induces a reversible expansion, which turns into an irreversible contraction once normal consolidation is reached. Cooling-heating cycles show a reduction in the domain of elastic response, which indicates a change in the material hardening state induced by temperature [10]. The magnitude of the reduction is controlled by the drained plastic thermal dilation of the material [4,8,2]. In undrained conditions, the measured thermal pressurization is higher than what would be expected from the usual thermal expansion of water always within the field of the reversible response of the material [2]. The origin of these anomalies is thought to arise from the anomalous behavior of water confined in nanometric pores. In particular, confined water is known to adopt a structure associated with hydration states, evidenced by XRD, and the transition between hydration states upon thermo-mechanical loading is analogous to martensitic transformations in shape memory alloys (SMA) [14]. Martensitic transformation in SMA is known to induce large latent energies [15,16], which suggests that similar large latent energies could arise in clays. The goal of the paper is to provide quantitative estimates of latent energies for realistic loading paths for boom and opalinus clays. Since measuring latent energy is extremely difficult, back-analysis of standard thermo-mechanical tests is proposed based on a rigorous thermodynamic framework.

The paper is organized as follows: section 2 introduces the energy balance of the saturated porous continuum and more specifically the latent energy terms. The detailed thermodynamic derivation of this energy balance is recalled in appendix A. Section 3, addresses the macroscopic constitutive laws involved in the thermal equation. In particular, a constitutive model for the clay porous solid that can quantitatively reproduce the typical thermo-mechanical behavior of clays is proposed. Section 4, deals with the validation of the proposed constitutive model by capturing the outcomes of the available experimental tests (drained and undrained heating, triaxial, oedometer) held under drained and undrained heating conditions. Section 5, quantifies the importance of latent energy relative to the total dissipated energy in the system.

2 | FIELD EQUATIONS OF THE POROUS MEDIUM

In the continuum description of a porous medium, latent energies are contributions to the energy balance that limit the release of heat during dissipative processes. These contributions are frequently neglected. To properly describe this phenomenon, one has to set the field equations (conservation laws) describing the continuum. A detailed derivation is provided in appendix A. In this section, we briefly recall the formal expression of the latent energy contributions in the energy balance.

Modeling the behavior of the porous medium requires expressing the conservation laws that will govern the response of the open continuum. These are the mass conservation law (Eq.A3), the energy conservation law (Eq.A4) and the generalized Newton's third law (momentum balance Eq.A11) for the open continuum. Even though these laws are well known, a thermodynamic formulation is essential in thermo-mechanical scenarios since it provides the proper couplings between the phases of the saturated porous continuum [9]. The first law of thermodynamics states the conservation of internal energy. For a saturated porous medium, the total internal energy involves two contributions: one for the fluid phase $\left(\vartheta_f e_f\left(\phi, s_f\right) = \frac{E_f}{M_s}\right)$ and one for the solid phase $\left(e_s\left(\varepsilon_{ij}, \phi, s_s, \chi_{ij}\right)\right)$, where we refer to specific internal energy per unit mass with $\vartheta_f = M_f/M_s$ the ratio of fluid and solid mass in the porous medium, E_f is the internal energy of the fluid, ϕ the porosity, s_f and s_s the specific entropies of the fluid and solid phases, respectively, ε_{ij} the strain components (small deformations are assumed herein), and χ_{ij} internal variables (strain-like) that account for the non-reversible behavior of the medium. In field and laboratory conditions, the fluid and solid phases are exchanging energy and volume (porosity) so that the two phases are in thermal and mechanical equilibrium and share the same temperature T and pore pressure P. The thermodynamic potential minimum in such conditions is not the internal energy, but the Legendre transform corresponding to the sum of the Helmholtz free energy, f_s, of the solid and the Gibbs free enthalpy, $g_f = \frac{G_f}{M_f}$, of the fluid: $f_s + \vartheta_f g_f = e_s + \vartheta_f e_f - \left(Ts_s + \vartheta_f\left(Ts_f - \frac{P}{\rho_f}\right)\right)$, with ρ_f the fluid density. This choice of thermodynamic potential makes it possible to formulate the conservation of energy in terms of temperature and fluid pressure. The first derivatives of this thermodynamic potential provide all the necessary constitutive relations and work-conjugated quantities describing the thermo-mechanical behavior of the porous medium (see Table A1, Eq.A14): stress conjugated to strain, entropies conjugated to temperature, and porosity conjugated to pressure. Usually, the compressibility of the solid material is much lower than that of the porous medium, and thus the overall volumetric deformations are mostly due to changes of porosity

$(\phi - \phi_0 \approx \varepsilon_{ii})$. As a consequence, one can remove one parameter from the thermodynamic description of the porous medium (porosity replaced by volumetric strain). In this simplified description, the quantity conjugated to strain becomes the effective stress $\sigma'_{ij} = \sigma_{ij} + P\delta_{ij} = \rho \left.\frac{\partial f_s}{\partial \epsilon_{ij}}\right|_{T,\chi_{ij}}$ (with δ_{ij} the Kronecker delta). In addition, thermo-mechanical hardening gives rise to non-recoverable energies that remains latent in the porous material once a transformation of the hardening state occurs (e.g., residual stresses due to differential thermal expansion). Following Picard[10], one can split the solid free energy into an elastic part f_e (recoverable) and a blocked part V (non recoverable): $f_s = f_e\left(\varepsilon_{ij} - \varepsilon^p_{ij}, T\right) + V\left(\chi_{ij}, T\right)$, where ε^p_{ij} are the components of the plastic strain. It is worth noting that the blocked energy may depend on temperature. This dependency is critical to explain the thermal hardening of clays and in particular the irreversible thermal contraction of normally consolidated clay, which is discussed in detail in section 3.3. Allowing the blocked energy to depend on temperature has a major consequence for the conservation of energy since it introduces a specific latent energy, often neglected in soil mechanics. The detailed expression of the free energy depends on the model considered and is the focus of the following section. With this thermodynamic description of the porous medium, the conservation of energy takes the form (see appendix A):

$$\frac{\partial T}{\partial t} = \frac{1}{c_p}\underbrace{\left(\underbrace{m_f T \left.\frac{-\partial\left(\frac{\phi}{m_f}\right)}{\partial T}\right|_P}_{L_p}\frac{\partial P}{\partial t} + \underbrace{\rho T \left.\frac{-\partial\left(\frac{\sigma'_{ij}}{\rho}\right)}{\partial T}\right|_{\varepsilon^e_{ij}}}_{\mathbf{L}^\varepsilon}\dot{\varepsilon}^e_{ij} - \underbrace{\rho T \left.\frac{-\partial\left(\frac{\zeta_{ij}}{\rho}\right)}{\partial T}\right|_{\chi_{ij}}}_{\mathbf{L}^\chi}\dot{\chi}_{ij}\right)}_{-L} + \frac{1}{c_p}\underbrace{\left(\tilde{x}_{ij}\dot{\varepsilon}^p_{ij} + \hat{x}_{ij}\dot{\chi}_{ij}\right)}_{d_s} + \underbrace{\frac{k_T}{c_p}}_{C_{th}} T_{,ii} \tag{1}$$

where m_f is the wet density of the porous fluid, ρ is the dry density of the porous medium that can be considered as constant $\left(\rho = \rho_0\right)$ under small strains, c_p is the specific heat capacity of the porous medium per unit of mass, $\zeta_{ij} = -\rho_0 \left.\frac{\partial V}{\partial \chi_{ij}}\right|_T$ are the thermodynamic quantities conjugated to the hardening variables, $\tilde{x}_{ij} = -\rho_0 \left.\frac{f_s}{\varepsilon^p_{ij}}\right|_{\varepsilon_{ij},\phi,T,\chi_{ij}}$ are the thermodynamic stresses conjugated to the plastic strains for the dry solid, $\hat{x}_{ij} = \frac{\sigma'_{ij}}{2} - \zeta_{ij} = -\rho_0 \left.\frac{f_s}{\chi_{ij}}\right|_{\varepsilon_{ij},\phi,T,\varepsilon^p_{ij}}$ are the thermodynamic stresses conjugated to the hardening variable for the dry solid, and k_T is the thermal conductivity of the porous continuum. In Eq.1, one can distinguish the mechanical dissipation (d_s), the thermal diffusivity (C_{th}), and the latent energy (L). The latent energy is the energy which remains stored in the porous medium. The first term is associated with the thermal expansion coefficient α_f of the fluid and is given by the expression $L_P = -m_f T\frac{\partial^2 g_f}{\partial T \partial P} = -3\alpha_f T\phi$. The term L_P can be interpreted as the opposite of the incremental heat released when compressing the fluid under isothermal conditions. The second term is the analogous contribution for the solid and can be related to the thermal expansion coefficient α of the solid: $L^\varepsilon_{ij} = -\rho_0 T\frac{\partial^2 f_s}{\partial T \partial \epsilon_{ij}} = -3\alpha T\frac{p'}{\kappa_\epsilon}\delta_{ij}$ (see Eq.B31). The term L^ε_{ij} can be interpreted as the opposite of the incremental heat released when changing the effective stress σ'_{ij} under isothermal conditions. Finally, the third latent heat is associated with the transformation of the hardening state given as a function of the plastic thermal expansion coefficient α_p of the solid: $L^\chi_{ij} = -\rho_0 T\frac{\partial^2 V}{\partial T \partial \chi_{ij}} = 3\alpha_p T\frac{p_\zeta}{\upsilon_\epsilon}\delta_{ij}$ (see Eq.B31). The term L^χ_{ij} can be interpreted as the heat absorbed when changing the hardening state of the material (plastic compression) under isothermal conditions. Unlike most materials, clays exhibit a plastic thermal contraction $\left(\alpha_p > 0\right)$ which means that part of the heat received is absorbed by thermal hardening.

Introducing the explicit expressions of the latent energies in Eq.1 and of the dissipation rate of the skeleton, the rate of heat received by the porous medium $\dot{Q} = c_p\frac{\partial T}{\partial t} - k_T T_{,ii}$ is given by:

$$\begin{aligned}\dot{Q} &= \left(\phi T 3\alpha_f\right)\frac{\partial P}{\partial t} + \left(T3\alpha\frac{p'}{\kappa_\epsilon}\delta_{ij}\right)\dot{\varepsilon}^e_{ij} + \left(T3\alpha_p\frac{p_\zeta}{\upsilon_\epsilon}\delta_{ij}\right)\dot{\chi}_{ij} + \tilde{x}_{ij}\dot{\varepsilon}^p_{ij} + \left(\frac{\sigma'_{ij}}{2} - \zeta_{ij}\right)\dot{\chi}_{ij} \\ &= \underbrace{\left(\phi T 3\alpha_f\right)\frac{\partial P}{\partial t} + \left(T3\alpha\frac{p'}{\kappa_\epsilon}\delta_{ij}\right)\dot{\varepsilon}^e_{ij} + \left(T3\alpha_p\frac{p_\zeta}{\upsilon_\epsilon}\delta_{ij}\right)\dot{\chi}_{ij}}_{-L} + \underbrace{\frac{p_0}{2}\sqrt{\left(\frac{\dot{\varepsilon}^p_v + \dot{\chi}}{2}\right)^2 + M^2_\epsilon\dot{\varepsilon}^{p^2}_s}}_{d_s}\end{aligned} \tag{2}$$

The choice made for the layout of the Gibbs energy density function of the solid phase (see Eqs.B28-B29) implicitly leads to the equality $\chi_{ij} = \epsilon^p_{ij}$, thus the fourth and the fifth terms in Eq.2 reduced to the usual dissipation rate $x_{ij}\dot{\epsilon}^p_{ij}$. Eq.2 provides an energy balance in which the sign of $\dot{Q}$ is determined by the respective weights of d_s and L. If the respective weights are such that $d_s > L$ the heat balance produces an exothermic reaction. On the contrary, if $d_s < L$ the work process produces an endothermic reaction.

Of particular interest is the influence of the latent energy terms on the temperature rise during thermo-hydro-mechanical stimulation of clays. Typical situations of interest vary depending on the drainage conditions of the interstitial fluid and on the thermo-mechanical loading paths and history. The drainage conditions can change from a transient regime characterized by an evolutionary pore pressure $\frac{\partial P}{\partial t} \neq 0$ (the most extreme being undrained conditions) to a stationary regime characterized by a constant pore pressure $\frac{\partial P}{\partial t} = 0$ (i.e., drained conditions). Some of the most commonly studied thermo-mechanical paths are isotropic, oedometric and triaxial heating. The first one is a non-isothermal test in which the sample constrained at a given stress level is heated, and the generated volumetric deformation is measured (contraction or expansion depending on the loading history). The second and third tests (oedometric and triaxial heating) are performed under isothermal conditions at different constant temperatures (i.e. the heating, or cooling, is applied before the mechanical load). In this paper, we will evaluate the importance of latent energy for these particular tests.

3 | A THERMO-MECHANICAL CONSTITUTIVE MODEL FOR CLAYS

In this section, we propose a formulation of the thermodynamic potential describing the porous medium. The validity of the proposed model is limited to ranges of temperature which do not cause a phase-change of the water, i.e. temperatures spanned between the freezing and boiling points. The model considers only rate-independent soil. The authors acknowledge that creep effects may be significant mainly after heating stages at a constant temperature[17,18]. However, in the short-term (i.e., days) Cui et al.[17] have shown an estimate of creep vs. consolidation $\left(\text{at a rate } 5.1 \cdot 10^{-4} \frac{\text{MPa}}{\text{min}}\right)$, over 72 hs., of 0.01% to 2%. This work neglect potential effects of creep and thus the results are valid for loading over short time scales. However, for long-term analysis accounting for creep would be important.

3.1 | The unusual thermo-mechanical behavior of clays

Unlike other materials, when clays are subjected to cycles of heating-cooling one observes a particular response that changes according to the drainage conditions. If drained conditions prevail when heated, clays exhibit an expansion if the material is over-consolidated (OCR > 1). This expansion is more significant for materials that exhibit a greater drained thermal dilation coefficient. This behavior persists until the material response becomes irreversible and the volumetric strains turns into a compaction. If instead, undrained conditions prevail when heated, clays develop a significant pore fluid pressurization, larger than that expected from the usual water thermal expansion. This unusual thermo-mechanical response is generally attributed to the high confinement of water in clay nanopores[2,13].

Several works have been proposed to model those anomalies within the framework of elasto-plasticity, in particular Hueckel and Borseto[19], Graham et al.[20], and Abuel-Naga et al.[21,22]. In most of them the common feature was to assume a reduction of the yield surface as temperature increases. Cui et al.[5] and Hong et al.[23], instead, consider an additional thermo-plastic mechanism that allows for the generation of irreversible thermal strains, even at high over-consolidation ratios. An interesting description, though, is the thermodynamic framework proposed by Picard[10] which considers a unique plastic mechanism but introduces a temperature-dependent blocked energy. It was observed that the proposed blocked energy captures very well the response of normally consolidated clays and strongly over-consolidated clays under heating-cooling cycles. Nonetheless, for clay samples at intermediate over-consolidation ratios, an additional constitutive assumption is needed since the typical response (initial reversible expansion followed by an irreversible contraction) cannot be captured within the framework of Picard. Figure 1 shows the results of thermal tests held on Boom-clay under drained isotropic conditions reported in Sultan[24] and the response of the model proposed by Picard[10], defined by (a) an elastic domain characterized by the material constants: κ^e the slope of the isotropic compression line, G the shear modulus and α the drained thermal expansion coefficient (see Table 1), and (b) a limit temperature-sensitive surface of Cam-clay type[10] $f^y = \frac{q^2}{M^2_\epsilon} + p'\left[p - p_c\left(\chi, T\right)\right]$.

To overcome this issue, we propose to re-formulate the model within the framework of bounding plasticity[25] which has been successfully used in scenarios in which the material history is uncertain. The blocked energy proposed by Picard[10] for clays thermo-mechanically loaded within this framework is enhanced by a multiplicative factor proportional to the mean yield stress at bounding and a radial distance between the true stresses (i.e. the current stress state) and the stresses at bounding state. This enhancement allows to properly model the response of clays at different over-consolidation ratios. Furthermore, the plastic flow of the rate of irreversible strains in the thermodynamic stress space, space that emerges as a direct consequence of considering the blocked energy, remains associated. As a consequence, this approach preserves the principle of maximal dissipation and thus the strict thermodynamic formulation of Picard's model.

3.2 | Fluid Phase

Clays are porous materials with significant void ratio, even higher than one in some cases. This means that the volume of water is quite significant in saturated clays. The properties and behavior of water in clay often differ from those observed in free water in a large reservoir. This is generally attributed to water adsorption[26,27]. Experimental evidences show that the first layers of water molecules near the clay mineral surfaces have unusual properties, different from bulk water, such as density, thermal expansion, and compressibility[28]. Recent advances in micromechanics and confined fluid properties address those anomalies by introducing new concepts such as water disjoining pressure, which shed light on the physics behind the complex mechanics of clay[29,30,13]. Yet, these approaches are usually quite complex and of limited transferability for investigations at larger scales. Alternatively, a reasonable approach consists in considering a usual description of the interstitial water, but with adapted thermo-mechanical moduli. We consider the water in the pores as a single component fluid that verifies the Gibbs-Duhem relation[31] $d\mu = \frac{dP}{\rho_f} - s_f dT$, with μ the chemical potential. This relation provides a direct route to formulate the Gibbs free enthalpy per unit mass g_f, since, by extensivity of a fluid, $dg_f = d\mu$. Following this relation, the thermo-mechanics of the fluid is fully described with only three parameters: the bulk modulus $\frac{1}{K_f} = -\rho_f \left.\frac{\partial(1/\rho_f)}{\partial P}\right|_T$, the thermal expansion $\alpha_f = \left.\frac{\rho_f}{3}\frac{\partial(1/\rho_f)}{\partial T}\right|_P = -\left.\frac{1}{3\rho_f}\frac{\partial s_f}{\partial P}\right|_T$, and the volumetric heat capacity at constant pressure $c_f^p = T\left.\frac{\partial s_f}{\partial T}\right|_P$. Integrating with respect to temperature and pressure, assuming constant fluid properties and small changes of density and temperature, one obtains the following state equations for the density and entropy:

$$\begin{aligned} \frac{1}{\rho_f} - \frac{1}{\rho_{f0}} &= -\frac{P-P_0}{\rho_{f0}K_f} + \frac{3\alpha_f}{\rho_{f0}}\left(T-T_0\right) \\ s_f - s_{f0} &= -\frac{3\alpha_f}{\rho_{f0}}\left(P-P_0\right) + \frac{c_f^P}{T_0}\left(T-T_0\right) \end{aligned} \tag{3}$$

where ρ_{f0} and s_{f0} are the fluid density and entropy at $P = P_0$ and $T = T_0$. Further integration of the Gibbs-Duhem equation provides the expression of the Gibbs free enthalpy of the fluid:

$$g_f = g_{f0} + \left(P-P_0\right)\left(\frac{1}{\rho_{f0}} - \frac{\left(P-P_0\right)}{2\rho_{f0}K_f}\right) + \frac{3\alpha_f}{\rho_{f0}}\left(P-P_0\right)\left(T-T_0\right) - \left(T-T_0\right)\left(s_{f0} + \frac{c_f^p\left(T-T_0\right)}{2T_0}\right) \tag{4}$$

where g_{f0} is the Gibbs free enthalpy at $P = P_0$ and $T = T_0$.

3.3 | Solid phase

For thorough investigations, one has to consider a 'realistic' description of the porous solid, i.e., a description that captures the experimental thermo-mechanics. Drained experiments provide the constitutive relations describing the behavior of the porous solid. The expression of the corresponding thermodynamic potential can be build by multiple integration of the differential form of the constitutive relations. Note that thermodynamic consistency requires that these differential forms satisfy the symmetry stated by the Maxwell's relations of the thermodynamic potential. In this section, we follow this strategy to choose an appropriate modeling of the solid. Traditionally, incremental constitutive relations of geomaterials have been stated in terms of stress increments $\left(\text{e.g. } d\varepsilon_v^e = \frac{\kappa}{p'}dp'\right)$. In this case, the corresponding thermodynamic potential minimum at equilibrium is the Gibbs energy density g_s, which is related to the Helmholtz free energy f_s according to the Legendre transform $g_s = f_s - \frac{1}{\rho}\sigma'_{ij}\varepsilon_{ij}$. Limiting ourselves to isotropic porous media, the thermodynamic state of the porous solid under controlled stress could be entirely defined[32] by the mean effective stress $p' = \frac{1}{3}\sigma'_{ij}\delta_{ij}$, the deviatoric stress $q = \sqrt{\frac{3}{2}s_{ij}s_{ij}}$ (with $s_{ij} = \sigma'_{ij} - p'\delta_{ij}$), the temperature T, and the internal hardening variables $\boldsymbol{\chi}$. Among the internal variables $\boldsymbol{\chi}$, we distinguish the volumetric and deviatoric plastic strains $\varepsilon_v^p = \varepsilon_{ii}^p$ and $\varepsilon_s^p = \sqrt{\frac{2}{3}\epsilon_{ij}^p\epsilon_{ij}^p}$ (with $\epsilon_{ij}^p = \varepsilon_{ij}^p - \frac{1}{3}\varepsilon_{ii}^p$) and, following Picard[10], we introduce a single additional variable χ

(detailed later) which serves as a kinematic hardening parameter. As in section 2, we can separate the elastic and blocked energies following the principle of separation of energies[33], but the Legendre transform from f_s to g_s adds a cross contribution between the stresses p' and q and the internal variables ε_v^p, ε_s^p, and χ[34]: $g_s\left(p',q,T,\boldsymbol{\chi}\right)=g_e\left(p',q,T\right)+V\left(\chi,T\right)+L\left(p',q,\varepsilon_v^p,\varepsilon_s^p,\chi\right)$. The expression of L depends on the choice of hardening variable χ and will be detailed later on.

g_e corresponds to the recoverable elastic energy upon unloading, whereas V represents the blocked elastic energy, which is not recovered upon unloading. It is widely accepted that the origin of the blocked energy V is due to the non-homogeneous nature of the strains held at micro-structural level and that it is common in most geomaterials[33]. Because of the heterogeneity of the micro-structure, thermal loading and plasticity induce residual strains and stresses throughout the clay particles and the associated energy is blocked energy. In addition, in the particular case of clays, hydration transitions within clay layers (change of number of adsorbed water layer) is also a form of blocked energy, analogous to phase transitions in martensitic materials[13]. Blocked energy is usually considered as a function of the hardening variables, but, in the case of clays, Picard[10] suggests to consider it also as a function of temperature. A peculiarity of the drained thermo-mechanical response of clays is the irreversible thermal contraction (see Fig. 1). An irreversible behavior is observed under constant effective stress, which suggests that the pre-consolidation pressure p_c is affected by temperature. Since for critical state models p_c depends directly on the blocked energy $\left(\frac{p_c}{2}=p_\zeta=\frac{-\partial V}{\partial\chi}\right)$[35], this justifies the choice of Picard: $V\left(\chi,T\right)$.

Elastic Gibbs energy density g_e

The expression of the elastic Gibbs energy density $g_e\left(p',q,T\right)$ can be obtained by integration of the associated constitutive laws. It is generally assumed that the shear elastic behavior is not coupled with the compressive and thermal behaviors, so that a complete thermodynamic description requires only 4 moduli: the bulk modulus $K\left(\frac{1}{K}=-\rho_0\left.\frac{\partial^2 g_e}{\partial p'^2}\right|_{q,T}\right)$, the shear modulus $G\left(\frac{1}{3G}=-\rho_0\left.\frac{\partial^2 g_e}{\partial q^2}\right|_{p',T}\right)$, the thermal expansion $\alpha\left(\alpha=-\frac{1}{3}\left.\frac{\partial^2 g_e}{\partial p'\partial T}\right|_{T}\right)$, and the specific heat capacity at constant stress c_s^e $\left(c_s^e=-T\left.\frac{\partial^2 g_e}{\partial T^2}\right|_{p',q}\right)$. It is known that the elastic behavior of clays is non-linear when subjected to mechanical loads[36]. The bulk modulus K is not constant but depends on the level of stress. Following the well-accepted modified Cam-clay model, $\frac{1}{K}=\frac{\kappa_\epsilon}{p'}$ where κ_ϵ is a material parameter that is usually obtained as the slope of the isotropic compression line (ICL) in the plane $e-\ln\left(p'\right)$ divided by $\left(1+e_0\right)$. Instead, the shear modulus G is often assumed constant, even though some non linearity may arise with large deformations[37]. In this work, the thermal deformations of interest are considered small, i.e. limited to a few percent, so it can be considered constant. The elastic thermo-mechanical coupling is characterized by the drained thermal expansion α. The modeling of elastic thermal expansion is a subject of debate, since experimental values are anomalously high for clays and may depend on temperature, which is generally attributed to the presence of bound water (see section 3.1). Yet, a constant thermal expansion α provides reasonable predictions with respect to experiments, even though the value of α to consider may well exceed conventional values for solids. Accordingly, Picard[10] proposes to consider a thermal expansion independent of stress and temperature, and we follow this choice in the present work. Finally, the heat capacity c_s^e is also generally considered constant (Dulong-Petit law). Accordingly, the incremental constitutive laws describing thermo-mechanical behavior of the porous solid are:

$$\begin{aligned} d\varepsilon_v^e &= \frac{\kappa_\epsilon}{p'}dp'-3\alpha dT \\ d\varepsilon_s^e &= \frac{1}{3G}dq \\ \rho_0 ds_s^e &= -3\alpha dp'+\rho_0\frac{c_s^e}{T}dT \end{aligned} \tag{5}$$

By integration of these constitutive laws, assuming small changes of dry density $\rho=\rho_0$ and temperature T, one readily obtains the expression of the elastic Gibbs energy density:

$$g_e\left(p',q,T\right)=-\frac{p'}{\rho_0}\kappa_\epsilon\left(\ln\left(\frac{p'}{p_0}\right)-1-\frac{3\alpha}{\kappa_\epsilon}\left(T-T_0\right)\right)-\frac{\left(q-q_0\right)^2}{6\rho_0 G}-\left(T-T_0\right)\left(s_{s0}^e+\frac{c_s^e\left(T-T_0\right)}{2T_0}\right) \tag{6}$$

where s_{s0}^e is the specific entropy associated with the elastic behavior of the porous solid at $p'=p_0$, $q=q_0$, and $T=T_0$.

Blocked energy V

The expression of the blocked energy density $V(\chi, T)$ can be obtained by the integration of the suitable hardening law. The laboratory tests carried out by Campanella[38], Baldi[39], Delage[4] concluded that an enlargement of the material plastic limit occurs after a heating-cooling cycle. The results of these tests suggest a model of thermal hardening for which the plastic limit p_c evolves according to $p_c = p_c\left(a\chi - b\left(T - T_0\right)\right)$. In particular, it has been shown that the thermal hardening law proposed by Picard[10] $p_c = p_{c0}\exp\left(\frac{\chi - 3\alpha_p(T-T_0)}{\upsilon_\epsilon}\right)$, captures well the thermo-mechanical paths of standard laboratory tests with temperature control (isotropic, oedometer, triaxial). In this law, α_p is the plastic drained thermal expansion coefficient and χ is an internal strain-like variable, which, due to the associativity of the plastic flow in the thermodynamic stress space, can be assumed as equal to the volumetric plastic strain $\chi = \varepsilon_v^p$. Then, the thermodynamic behavior of the material with thermal hardening needs 3 moduli: the bulk modulus of material hardening $K^p = -\rho_0\left.\frac{\partial^2 V}{\partial \chi^2}\right|_T$, the specific heat capacity associated to the blocked energy $c_s^b - 3\alpha_p T_0\frac{L_\chi}{T} = -T_0\left.\frac{\partial^2 V}{\partial T^2}\right|_\chi$, and the latent energy of hardening state transformation $\frac{L_\chi}{T} = -\rho_0\frac{\partial^2 V}{\partial T\partial\chi}$. The bulk modulus of material hardening is a pressure dependent modulus $K^p = \frac{p_\zeta}{\upsilon_\epsilon}$ where p_ζ is the mean back stress and $\upsilon_\epsilon = \frac{\kappa^p - \kappa^e}{1+e_0}$ is related to the slopes of the isotropic and normal compression lines in the $e - \ln p'$ plane, the thermoplastic-mechanical coupling is characterized by the plastic drained thermal expansion α_p, c_s^b is the specific heat capacity associated to the blocked energy at null latency saturation condition, considered constant, and L_χ is the latent energy of hardening state transformation. Accordingly, the incremental complementary constitutive relations describing the thermo-mechanical hardening behavior are:

$$\begin{aligned}\dot{p}_\zeta &= \frac{p_{c0}}{2\upsilon_\epsilon}\exp\left(\frac{\chi - 3\alpha_p\left(T-T_0\right)}{\upsilon_\epsilon}\right)\left(\dot{\chi} - 3\alpha_p\dot{T}\right) = \frac{p_\zeta}{\upsilon_\epsilon}\dot{\chi} + \frac{L_\chi}{T}\dot{T}\\ \rho_0\dot{s}_s^b &= \frac{L_\chi}{T}\dot{\chi} + \left(\rho_0\frac{c_s^b}{T_0} - 3\alpha_p\frac{L_\chi}{T}\right)\dot{T}\end{aligned} \tag{7}$$

Note, in particular, that the Maxwell relations for $V(\chi, T)$ imposes a relation between the latent energy and the back stress $\left(\frac{L_\chi}{T} = \left.\frac{\partial p_\zeta}{\partial T}\right|_\chi\right)$ which implies that the latent energy L_χ is involved in the evaluation of the back stress evolution under temperature changes. As a consequence, considering a kinematic hardening implies that not all plastic work developed during a thermomechanical load will be dissipated in heat form, but part of it will remain blocked in the material. By double integration of these constitutive laws and as before assuming small changes of dry density and temperature T, it is straightforward to obtain the blocked energy density:

$$V(\chi, T) = -\frac{\upsilon_\epsilon p_{c0}}{2\rho_0}\exp\left(\frac{\chi - 3\alpha_p\left(T-T_0\right)}{\upsilon_\epsilon}\right) - \left(T - T_0\right)\left(s_{s0}^b + \frac{c_s^b\left(T-T_0\right)}{2T_0}\right) \tag{8}$$

where s_{s0}^b is the specific entropy associated with the blocked energy at $p' = p_0$, $q = q_0$, and $T = T_0$.

Total Gibbs energy density g_s

The last term of the Gibbs energy density g_s is the term $L\left(p', q, \varepsilon_v^p, \varepsilon_s^p, \chi\right)$ arising from the contribution of the plastic strains and internal variable in the Legendre transform of f_s. Since the chosen internal variable $\chi = \varepsilon_v^p$ models a kinematic hardening, the expression of L that ensures that the total strain in the sum of the elastic and plastic strains is given by (see appendix B):

$$L\left(p', q, \varepsilon_v^p, \varepsilon_s^p, \chi\right) = -\frac{1}{\rho_0}\left(\frac{p'}{2}\left(\varepsilon_v^p + \chi\right) + q\varepsilon_s^p\right) \tag{9}$$

Combining Eqs. (6), (8), and (9), the total Gibbs density potential g_s of the porous solid is:

$$\begin{aligned}g_s = &-\frac{p'}{\rho_0}\kappa_\epsilon\left(\ln\left(\frac{p'}{p_0}\right) - 1 - \frac{3\alpha}{\kappa_\epsilon}\left(T-T_0\right)\right) - \frac{\left(q-q_0\right)^2}{6\rho_0 G} - \left(T-T_0\right)\left(s_{s0} + \frac{c_s\left(T-T_0\right)}{2T_0}\right)\\ &-\frac{1}{\rho_0}\left(\frac{p'}{2}\left(\varepsilon_v^p + \chi\right) + q\varepsilon_s^p\right) - \frac{\upsilon_\epsilon p_{c0}}{2\rho_0}\exp\left(\frac{\chi - 3\alpha_p\left(T-T_0\right)}{\upsilon_\epsilon}\right)\end{aligned} \tag{10}$$

where $s_{s0} = s^e_{s0} + s^b_{s0}$, $c_s = c^e_s + c^b_s$. The complete set of constitutive equations describing the total volumetric and deviatoric strains ε_v and ε_s, the total entropy s_s, and the thermodynamic forces $\tilde{p}_x$, q_x and $\hat{p}_x$ conjugated to the plastic strains and to the internal variable are obtained by derivation of g_s:

$$
\begin{aligned}
\varepsilon_v &= -\rho_0 \left.\frac{\partial g_s}{\partial p'}\right|_{q,T,\varepsilon^p_v,\varepsilon^p_s,\chi} = \underbrace{\kappa_\epsilon \ln\left(\frac{p'}{p_0}\right) - 3\alpha\left(T-T_0\right)}_{\varepsilon^e_v} + \frac{1}{2}\left(\varepsilon^p_v + \chi\right) \\
\varepsilon_s &= -\rho_0 \left.\frac{\partial g_s}{\partial q}\right|_{p',T,\varepsilon^p_v,\varepsilon^p_s,\chi} = \underbrace{\frac{q-q_0}{3G}}_{\varepsilon^e_s} + \varepsilon^p_s \\
s_s &= -\left.\frac{\partial g_s}{\partial T}\right|_{p',q,\varepsilon^p_v,\varepsilon^p_s,\chi} = s^e_{s0} - \frac{3\alpha}{\rho_0}p' + \frac{c^e_s}{T_0}\left(T-T_0\right) + \underbrace{s^b_{s0} + \frac{c^b_s}{T_0}\left(T-T_0\right) - \frac{3\alpha_p p_{c0}}{2\rho_0}\exp\left(\frac{\chi - 3\alpha_p\left(T-T_0\right)}{\upsilon_\epsilon}\right)}_{s^b_s} \\
\tilde{p}_x &= -\rho_0 \left.\frac{\partial g_s}{\partial \varepsilon^p_v}\right|_{p',q,T,\varepsilon^p_s,\chi} = \frac{p'}{2} \\
q_x &= -\rho_0 \left.\frac{\partial g_s}{\partial \varepsilon^p_s}\right|_{p',q,T,\varepsilon^p_v,\chi} = q \\
\hat{p}_x &= -\rho_0 \left.\frac{\partial g_s}{\partial \chi}\right|_{p',q,\varepsilon^p_v,\varepsilon^p_s,T} = \frac{p'}{2} - \underbrace{\frac{p_{c0}}{2}\exp\left(\frac{\chi - 3\alpha_p\left(T-T_0\right)}{\upsilon_\epsilon}\right)}_{p_\zeta}
\end{aligned}
\tag{11}
$$

where we highlight the split of the elastic and plastic strains (the usual split is recovered since $\chi = \varepsilon^p_v$), we identify the blocked entropy $s^b_s = -\left.\frac{\partial V}{\partial T}\right|_\chi$, and we identify the back stress $p_\zeta = -\rho_0 \left.\frac{\partial V}{\partial \chi}\right|_T$. The blocked entropy and the back stress arise from the blocked energy. They evolve only during the irreversible thermo-mechanical hardening and they remain blocked within the hardening state. These are not state functions of the system, since their values depend on the loading history. The sum of the two thermodynamic force $\tilde{p}_x$ and $\hat{p}_x$ gives the classical expression for the kinematic hardening of the Ziegler type[34]: $p_x = \tilde{p}_x + \hat{p}_x = p' - p_\zeta$. As will be discussed hereafter, the thermodynamic forces $\tilde{p}_x$, q_x, and $\hat{p}_x$ determine the hardening behavior, i.e., the evolution of the yield surface during plasticity. In particular, p_ζ controls the kinematic hardening and drives the evolution of the blocked energy at the origin of unusual latent energy L_χ involved in the transformation of the hardening state (see section 2). This latent energy is defined from the blocked entropy function s^b as $L_\chi = \rho_0 T \left.\frac{\partial s^b}{\partial \chi}\right|_T = T\frac{3\alpha_p p_\zeta}{\upsilon_\epsilon}$. The meaning of this latent heat becomes clear when considering the energy balance during irreversible processes: $\dot{Q} = \underbrace{\tilde{p}_x \dot{\varepsilon}^p_v + \hat{p}_x \dot{\chi} + q\dot{\varepsilon}^p_s}_{d_s} - L_\chi \dot{\chi}$. The sign of $\dot{Q}$ is determined by the respective weights of d_s and L_χ. If the respective weights of d_s and L_χ is such that the difference between them is positive, the plastic process produces an exothermic reaction (heat is released). On the contrary, if it is negative the plastic process produces an endothermic reaction (heat is absorbed). Introducing the latent energy in the differential form of the constitutive equations 11, we obtain:

$$
\begin{aligned}
\dot{\varepsilon}_v &= \frac{\kappa_\epsilon}{p'}\dot{p}' - 3\alpha\dot{T} + \frac{1}{2}\left(\dot{\varepsilon}^p_v + \dot{\chi}\right) \\
\dot{\varepsilon}_s &= \frac{1}{3G}\dot{q} + \dot{\varepsilon}^P_s \\
\rho_0 \dot{s}_s &= -3\alpha\dot{p}' + \left(\rho_0 \frac{c_s}{T_0} - 3\alpha_p \frac{L_\chi}{T}\right)\dot{T} + \frac{L_\chi}{T}\dot{\chi}
\end{aligned}
\tag{12}
$$

Plasticity

As discussed in section 3.1, we follow the framework of bounding plasticity[25]. Considering the limit surface of the Cam-clay model[36,35,32], a bounding surface distinct from the limit surface is introduced. The two surfaces are linked by a homothetic transformation such that the pre-consolidation pressure of the bounding surface is given by $p^B_c = \beta_0 p_c$ where $p_c(\chi, T)$ is the pre-consolidation pressure of the limit surface and β_0 is a scaling factor. In the thermodynamic space of kinematic hardening

the plasticity is associated (see Fig. 2) and, therefore, the hardening rule (rate of plastic strains and of the internal variable χ) is uniquely defined by the bounding surface $f^B\left(\bar{\bar{p}}_x, \bar{q}_x, \bar{\bar{p}}_x\right) = 0$, where $\bar{\bar{p}}_x$, $\bar{q}_x$ and $\bar{\bar{p}}_x$ are the image thermodynamic stresses in bounding surface. In bounding plasticity, one characterizes the bounding surface through a dual function $\bar{d}_s$, which is the scaling of the dissipation rate d_s of the Cam-clay model:

$$\bar{d}_s = \beta_0 d_s = \beta_0 \cdot \frac{p_c}{2}\sqrt{\left(\frac{\dot{\varepsilon}_v^p + \dot{\chi}}{2}\right)^2 + M^2 \dot{\varepsilon}_s^{p^2}} \tag{13}$$

where $M = 6\sin\phi'/(3-\sin\phi')$ is the slope of the critical state line in the plane of the true stresses $\left(p'-q\right)$ and ϕ' is the internal friction angle. Then, the existence of the bounding surface f^B is shown by the degenerate Legendre transformation $\lambda f^B = 0 = \bar{d}_s - \left(\bar{\bar{p}}_x \dot{\varepsilon}_v^p + \bar{\bar{p}}_x \dot{\chi} + \bar{q}_x \dot{\varepsilon}_s^p\right)$, where λ is the plastic multiplier. Therefore, the image thermodynamic forces on the bounding surface conjugated to the rates $\dot{\varepsilon}_v^p$, $\dot{\chi}$, and $\dot{\varepsilon}_s^p$ are obtained by invoking the complementary state equations (Tab. A2):

$$\begin{aligned}
\bar{\bar{p}}_x &= \left.\frac{\partial \bar{d}_s}{\partial \dot{\varepsilon}_v^p}\right|_{\dot{\chi},\dot{\varepsilon}_s^p} = \frac{\left(p_c^B\right)^2}{8\bar{d}_s}\left(\dot{\varepsilon}_v^p + \dot{\chi}\right) \\
\bar{\bar{p}}_x &= \left.\frac{\partial \bar{d}_s}{\partial \dot{\chi}}\right|_{\dot{\varepsilon}_v^p,\dot{\varepsilon}_s^p} = \frac{\left(p_c^B\right)^2}{8\bar{d}_s}\left(\dot{\varepsilon}_v^p + \dot{\chi}\right) \\
\bar{q}_x &= \left.\frac{\partial \bar{d}_s}{\partial \dot{\varepsilon}_s^p}\right|_{\dot{\varepsilon}_v^p,\dot{\chi}} = \frac{\left(p_c^B\right)^2 M^2}{4\bar{d}_s}\dot{\varepsilon}_s^p
\end{aligned} \tag{14}$$

Eliminating the rates of plastic strains and internal variable in the degenerate Legendre transform, the bounding surface equation is obtained:

$$f^B = \frac{\left(\bar{p}_x\right)^2}{\left(p_c^B/2\right)^2} + \frac{(\bar{q})^2}{M^2\left(p_c^B/2\right)^2} - 1 \tag{15}$$

where $\bar{p}_x = \bar{\bar{p}}_x + \bar{\bar{p}}_x$. Equation 15 represents a family of ellipses centered at the origin of the thermodynamic space of bounding forces $\left(\bar{p}_x - \bar{q}\right)$ with semi axis $p_c^B/2$ and $Mp_c^B/2$ in the $\bar{p}_x$ and $\bar{q}$ directions respectively. Figure 2, sketches this bounding plasticity model. For sake of readability, the term loading surface is used in the caption of the figure in a generalized sense.

Then, with the choice of hardening variable $\dot{\chi} = \dot{\varepsilon}_v^p$, the hardening flow rules are:

$$\begin{aligned}
\dot{\chi} = \dot{\varepsilon}_v^p &= \lambda \left.\frac{\partial f^B}{\partial \bar{p}_x}\right|_{\bar{q},p_c^B} = 2\lambda \bar{p}_x \\
\dot{\varepsilon}_s^p &= \lambda \left.\frac{\partial f^B}{\partial \bar{q}}\right|_{p_x,\bar{p}_c^B} = \frac{2\lambda \bar{q}}{M^2}
\end{aligned} \tag{16}$$

In addition to the scaling of the mean yield stress at bounding p_c^B, an additional scaling is introduced in bounding plasticity for the blocked energy as follows: $\tilde{V} = \frac{\beta_0}{\delta}V$, where δ is a scaling factor defined by the radial distance $\delta = \delta_0 - \sqrt{\left(\frac{\varepsilon_v^p}{a+\varepsilon_v^p}\right)^2 + \left(\frac{\varepsilon_s^p}{a+\varepsilon_s^p}\right)^2}$ in the plastic strain space, δ_0 is an initial distance and a is a material parameter. Thus, the enhanced blocked energy implies that the amount of plastic work that remains blocked is directly affected by δ. Therefore, the mean back stress is modified by the change of δ with respect to the volumetric plastic strain

$$p_\zeta = \rho_0 \left.\frac{-\partial \tilde{V}}{\partial \varepsilon_v^p}\right|_T = \frac{\rho_0\beta_0}{\delta}\left.\frac{-\partial V}{\partial \varepsilon_v^p}\right|_T + \rho_0 \frac{\beta_0 V}{\delta^2}\left.\frac{\partial \delta}{\partial \varepsilon_v^p}\right|_{\varepsilon_s^p} \tag{17}$$

The mean back stress p_ζ (Eq.17) introduces a yield surface of the material different from the limit surface (characterized by p_c) and from the bounding surface (characterized by p_c^B). In this way, we recover, with this bounding plasticity framework, a three-surface formulation which has been proposed for clays from energetic considerations[40,41,42]. Then, the fundamental relations between the thermodynamic and the true forces, in the current state and the bounding state are:

$$\begin{aligned} p_x &= p' - \underbrace{\left(\frac{\rho_0 \beta_0}{\delta} \left.\frac{-\partial V}{\partial \varepsilon_v^p}\right|_T + \rho_0 \frac{\beta_0 V}{\delta^2} \left.\frac{\partial \delta}{\partial \varepsilon_v^p}\right|_{\varepsilon_s^p} \right)}_{p_\zeta} \\ \bar{p}_x &= -\rho_0 \left.\frac{\partial \bar{g}_s}{\partial \varepsilon_v^p}\right|_{p',q,T,\varepsilon_s^p} = \bar{p}' - \underbrace{\rho_0 \beta_0 \left.\frac{-\partial V}{\partial \varepsilon_v^p}\right|_T}_{\bar{p}_\zeta} \end{aligned} \tag{18}$$

where $\bar{g}_s = g_e + \delta L + \beta_0 V$ is the scaled Gibbs energy density and $\bar{p}' = \delta p'$ is the true mean effective stress at bounding. It is noted that second order terms in the plastic strains $\left(p' \varepsilon_v^p \left.\frac{\partial \delta}{\partial \varepsilon_v^p}\right|_{\varepsilon_s^p} \right)$ have been neglected since they are very small (typically $\approx 10^{-14}$). Thus, unlike the mean back stress at current state, the mean back stress at bounding $\bar{p}_\zeta$ is independent of δ. Therefore, scaling Eq.18 (top) by δ is possible to obtain the mapping rule between the thermodynamic forces at the current state and the bounding state

$$\bar{p}_x = \delta p_x + \rho_0 \frac{\beta_0 V}{\delta} \left.\frac{\partial \delta}{\partial \varepsilon_v^p}\right|_{\varepsilon_s^p} \tag{19}$$

This mapping rule (Eq.19) is fundamental for the variational formulation of the model. It states that the thermodynamic forces at bounding state are not only scaled from the thermodynamic forces at the current state, but also shifted proportionally to the change of the radial distance with the plastic volumetric strain. The same analysis leads to the expressions for the deviatoric thermodynamic stresses q_x, at the current state, and $\bar{q}_x$, at the bounding state, respectively. By using the mapping rules Eqs.19 in the consistency condition at yielding state $df^y\left(p_x, q_x, \varepsilon_v^p, \varepsilon_s^p\right) = 0$, it is possible to derive the expressions for the plastic strain rates as a function of the generalized plastic modulus $H = H_p + H_\delta$, see appendix C.

$$\dot{\varepsilon}_v^p = \frac{d_f \dfrac{\partial f^y}{\partial p_x}}{H_p + H_\delta} \; ; \; \dot{\varepsilon}_s^p = \frac{d_f \dfrac{\partial f^y}{\partial q_x}}{H_p + H_\delta} \tag{20}$$

where $d_f = \frac{\partial f^y}{\partial p_x}\dot{p}' + \frac{\partial f^y}{\partial q_x}\dot{q}$, H_p is the plastic modulus at pure yielding $\left(\text{i.e. } f^y = f^B\right)$ and H_δ is the bounding modulus which increases H_p by a magnitude that depends on the radial distance δ and its derivatives. Unlike what happens in the classical formulation of bounding plasticity, the thermodynamic formulation of this framework naturally introduces a mapping rule of the plastic modulus variation in the domain between the yield and bounding surfaces.

It should be noted that in the proposed formulation the role of the limit surface is merely implicit since the only information needed is the loading history of the material $\left(p_c\right)$. This history is then used to evaluate the mean yield stresses at yield and bounding states. In summary, five new elements are introduced in this formulation ($\bar{d}_s$, $\tilde{V}$, $\bar{g}_s$, the mapping rule (Eq.19) and the derived bounding modulus H_δ). It provides the necessary ingredients to overtake the main limitations of Picard's model to quantitatively capture the response of clays at different initial states of over-consolidation.

4 | PARAMETERIZATION AND VALIDATION OF THE CONSTITUTIVE MODEL

This section is dedicated to the parameterization and validation of the proposed thermomechanical model. The model is calibrated to reproduce the behavior of Boom and Opalinus clays in the following thermo-mechanical tests: isotropic drained heating tests[24,4,5,2], drained oedometer tests at different temperatures[24,43], drained triaxial tests at different temperatures[39], and isotropic undrained heating tests[2,3]. Table 1 summarizes the model parameters for Boom and Opalinus clays, where α_f, α, and α_p are the linear thermal coefficients. Initial values of δ_0 are taken as the initial over-consolidation ratio.

4.1 | Drained heating tests

Figures 3 and 4 compare the experimental and modeled behavior of Boom and Opalinus clays, respectively, submitted to drained heating at constant effective pressure. Figure 3 (left) shows the comparison between the thermal volumetric strains reported by Delage et al.[4] for Boom clay to the predictions of the proposed model "B model". Initial conditions of the sample are: mean effective stress $p_0 = 3$MPa, temperature $T_0 = 23°$C, pre-consolidation $p_c^0 = 4$MPa and porosity $\phi_0 = 0.4$ (Picard[10]). The change of slope in the mechanical response corresponds to the transition from a reversible thermal expansion (α) to an irreversible thermal contraction ($-\alpha_p$), i.e., transition from elasticity to plasticity. This is reasonably captured by our model, although the actual transition from elasticity to plasticity is progressive and not sudden as in the model. It is noted that the progressive transition (i.e. nonlinear evolutions of strains) from elasticity to plasticity could be addressed in the proposed approach by selecting a new radial distance function δ. We also compare with the predictions of the well established models of Campanella[38] and Baldi[44]. Those are phenomenological models designed to fit experimental results, i.e., are not formulated in a thermodynamical framework. Our model proves as accurate as existing models, but it has the advantage to rely on a rigorous thermodynamical formulation, which is essential to address the issue of latent energy.

Figure 3 (right) shows the effect of over-consolidation ratio (OCR) on the response to drained heating tests for Boom clay. Experimental results are from Sultan[24], and are already discussed qualitatively in section 3.1 (Fig. 1). Initial conditions of the samples are: mean effective stresses $p_0 = 6$MPa, $p_0 = 3$MPa, $p_0 = 0.5$MPa, temperature $T_0 = 24°$C, pre-consolidation $p_c^0 = 6$MPa and porosity $\phi_0 = 0.4$ (Picard[10]). The predictions of our model compares well with experiments. Over-consolidation affects the point of transitions from reversible thermal expansion to irreversible thermal contraction. Yet, capturing accurately this transition is not straightforward. Our modeling strategy (combining blocked energy affected by temperature and bounding plasticity) proves capable and efficient to reproduce well the transitions at various OCR. It is noted that the case of highly over-consolidated clays with no observed thermal compaction is of little interest in the issue of latent heat since thermal compaction is the main source of latent heat.

Figure 4 shows the effect of a heating-cooling load on the response to drained heating test on Opalinus clay. Experimental results are from Monfared[2]. Initial conditions of the sample are: mean effective stress $p_0 = 2.2$MPa, temperature $T_0 = 25°$C, pre-consolidation $p_c^0 = 4$MPa and porosity $\phi_0 = 0.2$ (Wileveau[45]). As before for the over-consolidated samples of Boom, the model response captures well the laboratory results. Furthermore, the response is initially quasi-linear and reversible followed by an irreversible contraction up to the point where cooling starts.

The hysteresis behavior, observed during the cooling and re-heating branch, evidence a ratcheting effect that can be tackled by adopting a generalized nonlinear hardening law depending on an accumulative plastic strain[46]. This effect could be addressed in future studies.

4.2 | Oedometer drained tests

Figure 5 shows the results of oedometer tests held at different temperatures on samples of Boom-clay under drained conditions. The outcomes of the laboratory experiments are compared with the predictions of the proposed model. The laboratory tests, reported by Sultan[24], were performed as follows: the samples were initially isotropically loaded up to 4 MPa, then heated up to 100°C, and three samples were cooled down to 70°C, 40°C, and 23°C, respectively. Finally, all the samples were submitted to an oedometer test up to 6.37 MPa, 6.86 MPa, 8.45 MPa and 10 MPa, respectively. The initial stress states of the samples were calibrated according to the available data: for the sample heated up to T=100°C: $p_0 = 1.1$MPa; for the sample cooled down to T=70°C: $p_0 = 0.9$MPa; for the sample cooled down to T=40°C: $p_0 = 0.8$MPa; and for the sample cooled down to T=23°C: $p_0 = 0.7$MPa. The remaining initial conditions are common to all the samples: temperature $T_0 = 23°$C, pre-consolidation $p_c^0 = 4.6$MPa and porosity $\phi_0 = 0.4$. It is readily observed that the pre-consolidation pressure decreases with temperature. This phenomenon is a thermal hardening, which is accounted for in the proposed model by considering that blocked energy depends on temperature. This approach, allows to accurately capture the response of the over-consolidated material at various temperatures.

4.3 | Triaxial drained tests

Figure 6 shows the drained triaxial tests results of Boom clay at two different temperatures, reported by Baldi et al.[39]. The outcomes of the experiments are confronted to the predictions of the proposed thermomechanical model, with and without bounding plasticity. The triaxial loading is performed starting from an isotropic stress state at an effective pressure $p' = 2$ MPa,

which corresponds to an initial OCR = 2 (the pre-consolidation pressure of Boom clay at ambient temperature is estimated to 4 MPa). Initial conditions of the samples are: temperature $T_0 = 20°C$, pre-consolidation $p_c^0 = 4.0$MPa, and porosity $\phi_0 = 0.4$ (Picard[10]). Unidirectional vertical strain is applied while the horizontal stresses are maintained constant and the shear stress and volumetric strains are reported, for two temperatures: $T = 20°C$ and $T = 90°C$. It is important to note that, during heating, from $T = 20°C$ to $T = 90°C$, the response of the material remains elastic, i.e. no change of the mean yield stress was produced. In case of irreversible response during heating, the yield stress is expected to change according to the hardening law[10]. The triaxial loading reaches the plastic regime and loading-unloading cycles are performed. As observed in the oedometer test, the pre-consolidation pressure tends to decrease with temperature so that the plasticity begins earlier at 90°C than at 20°C.
However, the elastic moduli (slopes of elastic portions), and the hardening (slopes of plastic portions) seems little or not at all affected by temperature. Note that the sudden decrease of stress and strain at the end of the triaxial test at 20°C seems reminiscent of the onset of an instability / localization, which is beyond the scope of the present paper. Accordingly, we disregard this portion of the experimental curve at 20°C.
Confrontation with the proposed model provides reasonable predictions for the stress-strain curve. In particular, the use of bounding plasticity appears to improve significantly the predictions. The predictions for the volumetric strain, though, tend to overestimate the experimental results. We attribute this over-estimation to an excessive Poisson's ratio for the particular sample of Boom clay investigated in this test, possibly because of anisotropy or of an excessive bulk modulus. Moreover, the over-estimation tends to increase with the strain, which suggests that assuming a constant shear modulus G may be questionable at large strains. It is noted that in the absence of more detailed data sets in large strains (greater than 10%), no comparison was able to be performed beyond the axial strain of 6%.

4.4 | Undrained heating test

Undrained heating tests are not as common as drained heating tests. Outcomes of undrained heating tests performed on samples of Boom clay and Opalinus claystone were reported in Monfared[2,3]. The test consists in increasing the temperature of the sample from 25°C to 55°C (to 40°C in the samples of Boom clay) while maintaining the total pressure constant and preventing the drainage of the fluid. Heating induces an increase of pore pressure, which is measured. Slow heating ensures a homogeneous pore pressure distribution. Two samples of Boom clay were tested. The reported initial conditions (at laboratory test) are: porosity $\phi = 0.4$, total pressure $p = 3.25$ MPa and pore pressure $P = 1.0$ MPa. One of the samples was isotropically compressed up to total mean stress of 10 MPa before the heating. The compression was performed at constant temperature and under drained conditions so that the pore pressure remains equal to 1.0 MPa. The final pore pressures in each of the tests are 1.23 MPa (for the sample heated at $p = 3.25$ MPa) and 2.5 MPa (for the sample heated at $p = 10$ MPa), so that the effective pressure remains positive throughout the tests. Monfared[3] reports the pore pressure as a function of temperature, which we display in Fig.7 (left).

The sample of Opalinus claystone was heated from the initial conditions: porosity $\phi = 0.2$, total pressure $p = 4.1$ MPa and pore pressure $P = 2.2$ MPa, as determined in situ. The final pore pressure is 3.7 MPa, so that the effective pressure remains positive throughout the test. Monfared et al.[2] report the pore pressure as a function of temperature, which we display in Fig.7 (right). Poromechanical analysis of the undrained heating test is based on the thermal pressurization coefficient $\Lambda = \left.\frac{\partial P}{\partial T}\right|_{p,M_f}$ (see Monfared et al.[2], Rattez et al.[6]). Combining the tangent constitutive relations for the porous volume variation, the fluid density variation with respect to fluid pressure and temperature and the fluid mass $\left(M_f = \rho_f \phi \Omega_t\right)$, Monfared[2] recalls the general expression for the thermal pressurization coefficient Λ, under undrained condition $dM_f = 0$,

$$\Lambda = \frac{3\phi\left(\alpha_f - \alpha_s\right)}{S} \tag{21}$$

where α_s is the thermal dilation of the solid and $S = \frac{1}{K} - \frac{1}{K_s} + \phi\left(\frac{1}{K_f} - \frac{1}{K_s}\right)$ is the storage coefficient given in terms of the drained bulk modulus K, the bulk modulus of the solid K_s and the bulk modulus of the fluid K_f. The pore pressure of the undrained heating test is obtained by integrating equation 21. If the solid is assumed incompressible $\left(\frac{1}{K_s} = 0\right)$ Eq.21 (by Monfared) and the one proposed by Rattez[6] coincides. Expression 21 shows that the thermal pressurization coefficient is proportional to the mismatch of thermal expansion between the fluid and the solid phases. Yet, application to the undrained heating test of Opalinus clay and Boom clay significantly underestimate the experimental results (see Fig. 7b). Monfared et al.[2] attribute this discrepancy to the anomalous behavior of water adsorbed in clay, and suggest to consider a thermal expansion of water higher than the usual value. Following that strategy, we can predict correctly the thermal pressurization by considering a water thermal expansion of $3\alpha_f = 7.7 \cdot 10^{-4}\mathrm{K}^{-1}$ instead of the usual value $3\alpha_f = 3.8 \cdot 10^{-4}\mathrm{K}^{-1}$ in the range 25°C to 55°C (see Fig. 7). A more

accurate prediction is possible by considering a dependency of α_f on temperature, as done by Monfared et al.[2]. But, for sake of simplicity, we consider here a constant water thermal expansion, which already provides reasonable predictions with respect to the experimental data.

5 | ESTIMATION OF LATENT ENERGY

In this section, we provide quantitative estimates of latent energies for realistic loading paths for boom and opalinus clays obtained with the B model which has proven to properly capture laboratory tests (sec.4).
As we have seen, temperature changes are directly related to the latent energy. Eliminating the thermal diffusivity, the temperature change in the porous continuum (Eq. 1) can be re-expressed as:

$$\frac{\partial \mathrm{T}}{\partial \mathrm{t}} = \frac{1}{\mathrm{c_p}} \left(\mathrm{d_s} - \mathrm{L} \right) \tag{22}$$

Equation 22 reveals that the lower the work that remains latent in the porous medium, the greater the temperature change. In this section, we will quantify the fraction of plastic work that remains latent for various loading conditions. For this purpose, we will use the thermo-mechanical loading paths considered to validate the proposed thermo-mechanical model in section 4.

5.1 | Isotropic heating tests

In drained conditions, the latent energy of pore pressure state transformation is zero, while the latent energies of stress state transformation $\mathbf{L}^{\epsilon}$ and of hardening state transformation $\mathbf{L}^{\chi}$ are mobilized.
Figures 8 and 9 show the estimated work, which remains latent in samples of Boom clay and Opalinus clay, respectively, during the plastic yielding of the drained heating tests. It can be observed that, as the temperature in the porous medium increases, the work performed which remains latent in the medium increases. The latent energy at the beginning of the plastic yielding is higher in the samples with a higher over-consolidation ratio. In all the samples, the work performed, which remains latent in the porous medium under drained heating, ranges from 30% to 80%, which is very significant. The magnitude of the latent energy $\mathbf{L}^{\epsilon}$ is very small and of opposite sign compared to $\mathbf{L}^{\chi}$, the latent energy due to the thermal hardening characterized by α_p is the main physical origin of the phenomenon.
As a consequence, to consider the latent energy in the porous medium when it is in a drained configuration with increasing temperature is really important (e.g., long term nuclear waste storage).

5.2 | Oedometric heating tests

Figure 10 shows the computed work which remains latent in samples of Boom clay subjected to oedometer loading after going under a heating-cooling cycle. The percentage of work that remains latent appears very sensitive to the temperature from 40-50% at 100°C to 10-20% at 23°C.

Unlike what is observed in the drained heating tests, the percentage of work that remains latent in the samples during the oedometric load appears with a slightly decreasing tendency that implies a gradual rise of the mechanical dissipation due to mainly the deviatoric component of the plastic strain rate. The latent energy $\mathbf{L}^{\epsilon}$ is again lower than $\mathbf{L}^{\chi}$, but it is much more significant in magnitude compared to the value obtained in the isotropic drained heating tests, due to higher values of the mean effective stress.

5.3 | Triaxial heating tests

Figure 11 shows the estimated percentage of plastic work that remains latent in samples of Boom clay subjected to triaxial loading. The trend observed is similar to that reported in the oedometer tests but with a stronger decrease with plastic yielding. This stronger sensibility is due to the larger contribution of deviatoric strains to plasticity in the triaxial test whereas thermal hardening is a volumetric effect only. At room temperature, the percentage of plastic work that remains latent $\mathbf{L}^{\chi}$ is considerably lower than that estimated for the sample previously heated up to 90°C (almost one order of magnitude lower).

5.4 | Undrained heating-triaxial tests

An undrained configuration in a porous medium prevails when the thermo-hydro-mechanical loading is much faster than the characteristic time of fluid flow through the medium. In undrained conditions, all the components of the latent energy of the porous continuum (Eq.1) are mobilized, since changes of pore pressure is expected upon thermo-mechanical loading. Figures 12 and 13, show the estimated percentage of work that remains latent in samples of Boom clay and Opalinus claystone during undrained triaxial plastic yielding, that occurs after the undrained heating pressurization. These loadings do not correspond to the undrained heating experiments, but are fictitious plastic evolutions supposed to occurs after the undrained heating to provide an estimate of the latent energy of hardening transformation (since it can only be assessed for irreversible evolution and the undrained heating tests are reversible).

Figure 12 (top, right) shows that for the sample tested at a confined pressure of 3.25 MPa the latent energy at the onset of plastic triaxial shearing is about 45% and rapidly decreases as plastic yielding evolves. This trend is also observed for the latent energy components of pore pressure and hardening state transformations, which also have similar magnitudes. This result is quite different from the one observed in Fig.12 (bottom, right) for the sample confined at 10 MPa. In this case, the latent energy of pore pressure state transformation $\left(L_p\right)$ dominates over the hardening latent energy (L^χ) with an initial value of about 60% that quickly decrease as plastic yielding increases. This is the only test where this was observed. Such a scenario of high level confining pressure is typical of active seismic faults rich in clay (e.g. Aigion fault, Sulem[8]), with cores at depths of hundreds of meters and significant effective pressures (e.g. $p' = 11.4$ MPa, Sulem[8]).

Figure 13 shows that the percentage of latent heat of hardening state transformation decreases faster than both, the total latent energy and the latent energy of pore pressure state transformation, as plastic yielding increases. The latent energy of pore pressure state transformation slightly increases during plastic yielding up to a plastic strain of 0.1%. This slight increase coincides with a smooth decrease in the total latent energy. Decrease that becomes more pronounced later.

6 | DISCUSSION AND CONCLUDING REMARKS

In this paper, we provide estimates of latent energy contribution in the energy balance of thermally loaded clay. Because latent energies developed in mechanical tests are difficult to measure, an estimation from classical tests is possible by considering a back analysis based on a rigorous thermodynamical framework. In this framework, it is necessary to consider a constitutive model for clays that captures quantitatively the experimental behavior.

This motivated the development of a new THM model starting from the model proposed by Picard[10] combined with the framework of bounding plasticity which is critical to capture correctly the transition from reversible thermal expansion to irreversible thermal contraction observed in isotropic heating tests. The new THM model was calibrated and validated for Boom and Opalinus clays for drained and undrained heating tests, and for oedometer and triaxial tests at different temperatures. Once calibrated, the proposed THM model was used to estimate the latent energy contributions in the same tests. Our results tend to show that these contributions are very significant (tens of %). Such high latent energy may be critical for various geotechnical issues such as anticipating the temperature rise around nuclear wastes in deep geological storages (Delage[1]) or analyzing the stability of clayey faults (Stefanou[47]).

Our results suggest that 1) latent contribution is clearly dominated by the thermal hardening, 2) it increases with temperature, and 3) it decreases with deviatoric plastic strains. Considering latent energy appears important in the early stages of the plastic response of clays in both drained and undrained conditions. The sensitivity to temperature is the mostly visible in the drained heating test. The plastic work that remained latent ranges approximately from 30% to 80% and increases with plastic strain. Instead, the tests with an initial heating stage followed by oedometric or triaxial loadings showed a progressive decrease of the latent contribution with plastic strain. This decrease was more pronounced in the triaxial than in the oedometer tests because latent energy originates from the coupling between temperature and volumetric strain, and therefore more deviatoric strains (triaxial) reduces the relative latent contribution to plastic work. The same trend is obtained in the undrained heating-triaxial test, however the activation of the latent energy of pore pressure state transformation in undrained conditions increases the overall latent contribution.

The latent energy due to hardening appears clearly dominant. It is a peculiarity of clays since it is related to the irreversible thermal contraction α_p, which is not observed for most materials. Thermal contraction in clays is thought to originate from the dehydration of clay-layers at nanoscale (Brochard[14]). Dehydration generates very large contractions at the clay layer scale (typically 20%), and therefore explains the large magnitude of macroscopic thermal contraction of geo-materials containing a

significant amount of swelling clays (a few %). Our results show that the magnitude of the thermal contraction dramatically changes the contribution of latent energy to the energy balance whereas this contribution is negligible for most materials (no thermal hardening). The transition between dehydration states of clay-layers at nanoscale upon thermo-mechanical loading is analogous to martensitic transformations in shape memory alloys (Brochard[14]) which also show large latent contributions. This establishes an interesting parallel between two very different types of materials. Further investigation and experimental data is needed to consolidate these estimates (e.g, the effect of a generalized nonlinear hardening).

7 | ACKNOWLEDGMENTS

We gratefully acknowledge funding through the project TEAM2ClayDesicc from the French National Research Agency (Agence Nationale de la Recherche, contract ANR-14-CE05-0023). The author, I.S., would like to acknowledge the support of the European Research Council (ERC) under the European Union's Horizon 2020 research and innovation program (Grant agreement no. 757848 CoQuake). The corresponding author acknowledges Ms. Marta Woloszka for writing assistance and language editing.

References

1. Delage P, Cui Y, Tang A. Clays in radioactive waste disposal. *Journal of Rock Mechanics and Geotechnical Engineering* 2010; 2(2): 111–123. doi: 10.3724/sp.j.1235.2010.00111

2. Monfared M, Sulem J, Delage P, Mohajerani M. A laboratory investigation on thermal properties of the Opalinus claystone. *Rock Mechanics and Rock Engineering* 2011; 44(6): 735–747. doi: 10.1007/s00603-011-0171-4

3. Monfared M. *Couplages température-endommagement-perméabilité dans les sols et roches argileux*. PhD thesis. Ecole des Ponts ParisTech - ENPC, 6-8 Avenue Blaise Pascal, 77420 Champs-sur-Marne; 2012.

4. Delage P, Sultan N, Cui YJ. On the thermal consolidation of Boom clay. *Canadian Geotechnical Journal* 2000; 37(2): 343–354. doi: 10.1139/t99-105

5. Cui YJ, Sultan N, Delage P. A thermomechanical model for saturated clays. *Canadian Geotechnical Journal* 2000; 620: 607–620.

6. Rattez H, Stefanou I, Sulem J. The importance of Thermo-Hydro-Mechanical couplings and microstructure to strain localization in 3D continua with application to seismic faults. Part I: Theory and linear stability analysis. *Journal of the Mechanics and Physics of Solids* 2018; 115: 54–76. doi: 10.1016/j.jmps.2018.03.004

7. Rattez H, Stefanou I, Sulem J, Veveakis M, Poulet T. The importance of Thermo-Hydro-Mechanical couplings and microstructure to strain localization in 3D continua with application to seismic faults. Part II: Numerical implementation and post-bifurcation analysis. *Journal of the Mechanics and Physics of Solids* 2018; 115: 1–29. doi: 10.1016/j.jmps.2018.03.003

8. Sulem J, Lazar P, Vardoulakis I. Thermo-poro-mechanical properties of clayey gouge and application to rapid fault shearing. *International Journal for Numerical and Analytical Methods in Geomechanics* 2007; 31(3): 523–540. doi: 10.1002/nag.584

9. Hemp WS. Foundations of Solid Mechanics. Y. C. Fung. Prentice-Hall, New Jersey. 1965. 525 pp. Diagrams. £5.. *The Journal of the Royal Aeronautical Society* 1966; 70(663): 453–454. doi: 10.1017/S0001924000058632

10. Picard JM. *Écrouissage thermique des argiles saturées: application au stockage des déchets radioactifs*. Book. Ecole des Ponts ParisTech, 6-8 Avenue Blaise Pascal, 77420 Champs-sur-Marne; 1994.

11. Farren WS, Taylor GI. The Heat Developed during Plastic Extension of Metals. *Proceedings of the Royal Society A: Mathematical, Physical and Engineering Sciences* 1924; A107: 422–451. doi: 10.1098/rspa.1925.0034

12. Taylor GI, Quinney H. The Latent Energy Remaining in a Metal after Cold Working. *Proceedings of the Royal Society A: Mathematical, Physical and Engineering Sciences* 1934; 143(849): 307–326. doi: 10.1098/rspa.1934.0004

13. Brochard L, Honório T, Vandamme M, Bornert M, Peigney M. Nanoscale origin of the thermo-mechanical behavior of clays. *Acta Geotechnica* 2017; 12(6): 1261–1279. doi: 10.1007/s11440-017-0596-3

14. Brochard L. Expansion thermique anormale de l ' eau dans les argiles. In: L'Adsorption deJdlF. , ed. *7emes Journées de l'Association Française de l ' Adsorption*Association Française de l'Adsorption. ; 2018; Marseille.

15. Shaw JA, Kyriakides S. Thermomechanical Aspects of NiTi. *Journal of the Mechanics and Physics of Solids* 1995; 43(8): 1243–1281.

16. Armattoe KM, Bouby C, Haboussi M, Ben Zineb T. Modeling of latent heat effects on phase transformation in shape memory alloy thin structures. *International Journal of Solids and Structures* 2016; 88-89: 283–295. doi: 10.1016/j.ijsolstr.2016.02.024

17. Cui YJ, Le TT, Tang AM, Delage P, Li XL. Investigating the time-dependent behaviour of Boom clay under thermomechanical loading. *Geotechnique* 2009; 59(4): 319–329. doi: 10.1680/geot.2009.59.4.319

18. Li Y, Dijkstra J, Karstunen M. Thermomechanical creep in sensitive clays. *Journal of Geotechnical and Geoenvironmental Engineering* 2018; 144(11): 1–11. doi: 10.1061/(ASCE)GT.1943-5606.0001965

19. Hueckel T, Borsetto M. Thermoplasticity of saturaed clays: constitutive equations. *Journal of Geotechnical Engineering* 1990; 116(12): 1765–1777. doi: 10.1061/(ASCE)0733-9410(1990)116

20. Graham J, Tanaka N, Crilly T, Alfaro M. Modified Cam-Clay modelling of temperature effects in clays. *Canadian Geotechnical Journal* 2001; 38(3): 608–621. doi: 10.1139/cgj-38-3-608

21. Abuel-Naga, H. M., Bergado, D. T., Bouazza, A. and Ramana GV. Volume change behaviour of saturated clays under drained heating conditions: experimental results and constitutive modelling. *Canadian Geotechnical Journal* 2007; 44(8): 942–956.

22. Abuel-Naga, H. M., Bergado, D. T., Bouazza, A. and Pender M. Thermomechanical model for saturated clays. *Géotechnique* 2009; 59(3): 273–278.

23. Hong, P.Y., Pereira, J.M., Cui, Y.J. and Tang A. Mechanical and transport constitutive models for fractures subject to dissolution and precipitation. *International Journal for Numerical and Analytical Methods in Geomechanics* 2016; 40: 1059–1080. doi: 10.1002/nag

24. Sultan N, Delage P, Cui YJ. Temperature effects on the volume change behaviour of Boom clay. *Engineering Geology* 2002; 64(2-3): 135–145. doi: 10.1016/S0013-7952(01)00143-0

25. Dafalias, Yannis F HL. Bounding Surface Formulation of Soil Plasticity. In: G.N. P, , O.C. Z., eds. *Soil Mechanics -Transient and Cyclic Loads*John Wiley and Sons. 1982 (pp. 253).

26. Honorio T, Brochard L, Vandamme M. Hydration Phase Diagram of Clay Particles from Molecular Simulations. *Langmuir* 2017; 33(44): 12766–12776. doi: 10.1021/acs.langmuir.7b03198

27. Ferrage E, Lanson B, Michot LJ, Robert JL. Hydration Properties and Interlayer Organization of Water and Ions in Synthetic Na-Smectite with Tetrahedral Layer Charge. Part 1. Results from X-ray Diffraction Profile Modeling. *The Journal of Physical Chemistry C* 2010; 114(10): 4515–4526. doi: 10.1021/jp909860p

28. Low P. Nature and properties of water in montmorillonite-water systems. *Soil Science Society of America* 1979; 43(4): 651–658.

29. Dormieux L, Kondo D, Ulm FJ. *Microporomechanics*. Chichester, UK: John Wiley & Sons, Ltd. first edit ed. 2006

30. Murad MA, Moyne C. A dual-porosity model for ionic solute transport in expansive clays. *Computational Geosciences* 2008; 12(1): 47–82. doi: 10.1007/s10596-007-9060-z

31. Coussy O. *Mechanics and Physics of Porous Solids*. Chichester, UK: John Wiley & Sons, Ltd . 2010

32. Coussy O. *Poromechanics*. Chichester, UK: John Wiley & Sons, Ltd . 2003

33. Ulm, F.J. and Coussy O. *Mechanics and durability of solids*. Prentice Hall . 2003.

34. Collins, I.F. and Houlsby G. Application of thermomechanical principles to the modelling of geotechnical materials. *Proceedings of the Royal Society A: Mathematical, Physical and Engineering Sciences* 1997; 453(1964): 1975–2001. doi: 10.1098/rspa.1997.0107

35. Houlsby GT. *A Study of Plasticity Theories and Their Applicability to Soils*. PhD thesis. Cambridge, Cambridge, UK; 1981.

36. Roscoe, K.H. and Burland J. On the Generalised stress-strain behaviour of wet clay. In: Heyman J, Leckie F. , eds. *Engineering Plasticity*Cambridge University. Cambridge University Press; 1968; Cambridge: 535–609.

37. Borja RI, Tamagnini C, Amorosi A. Coupling plasticity and energy-conserving elasticity models for clays. *Journal of Geotechnical Engineering* 1997; 123(10): 948–957. doi: 10.1061/(ASCE)1090-0241(1997)123:10(948)

38. Campanella R.G. and Mitchell J. *Influence of temperature variations on soil behavior*. California: Berkeley: University of California, Institutie of Transportation and Traffic Engineering. Soil mechanics and Bituminous material research laboratory . 1968.

39. Baldi, G., Borsetto, M. and Pellegrini R. Medium scale laboratory tests for the interpretation of predictive models of the thermomechanical properties of clay barriers. *International workshop on thermo-mechanics of clays and clay barriers* 1993.

40. Hashiguchi K. Constitutive equations of elastoplastic materials with elastic-plastic transition. *Journal of Applied Mechanics, Transactions ASME* 1980; 102(2): 266–272. doi: 10.1115/1.3157581

41. Mroz, Z., Norris, V.A. and Zienkiewicz O. An anisotropic critical state model for soils subject to cyclic loading. *Geotechnique* 1981; 31: 451–469.

42. Stallebrass S. *The Effect of Recent Stress History on the Deformation of Over-consolidated Soils*. PhD thesis. City University, London, UK; 1990.

43. Horseman, S.T., Winter, M.G. and Entwistle D. *Geotechnical characterization of Boom clay in relation to the disposal of radioactive wate*. Commission of the European Communities . 1987

44. Baldi G, Hueckel T, Pellegrini R. Thermal volume change of mineral water system in low porosity clay. *Canadian Geotechnical Journal* 1988; 25(4): 807–825.

45. Wileveau Y. THM behaviour of host rock (HE-D) experiment: Progress report. Part 1.. tech. rep., Andra; 1/7, rue Jean Monnet, Parc de la Croix-Blanche, 92298 Châtenay-Malabry Cedex: 2005.

46. Lemaitre J, Chaboche JL. *Mechanics of Solid Materials*. Paris: Cambridge University Press . 1990

47. Stefanou I, Alevizos S. Fundamentals of bifurcation theory and stability analysis. *Modelling of instabilities and bifurcation in Geomechanics, ALERT geomaterials Doctoral School 2016* 2016.

48. Cekerevac C, Laloui L. Experimental study of thermal effects on the mechanical behaviour of a clay. *International Journal for Numerical and Analytical Methods in Geomechanics* 2004; 28(3): 209–228. doi: 10.1002/nag.332

49. Quinney, H. and Taylor G. The emission of the latent energy due to previous cold working when a metal is heated. *Proceedings of the Royal Society of London. Series A, Mathematical and Physical Sciences* 1937; 163(913): 157–181.

50. Baldi, G., Hueckel, T., Peano, A. and Pellegrini R. Developments in modelling of thermo-hydro-geomechanical behaviour of Boom Clay and clay-based buffer materials. tech. rep., ISMES; Luxembourg: 1991.

51. Houlsby, G.T. and Puzrin A. *Principles of Hyperplasticity*. London: Springer London . 2006

52. Liu H, Zou D, Liu J. Non-isothermal plasticity model for cyclic behaviour of soils. *International Journal for Numerical and Analytical Methods in Geomechanics* 2015; 32(March 2007): 189–213. doi: 10.1002/nag

53. Lund JW, Bjelm L, Bloomquist G, Mortensen AK. Characteristics, development and utilization of geothermal resources - A nordic perspective. *Episodes* 2008; 31(1): 140–147. doi: 10.18814/epiiugs/2008/v31i1/019

54. Ghabezloo S, Sulem J, Saint-Marc J. The effect of undrained heating on a fluid-saturated hardened cement paste. *Cement and Concrete Research* 2008; 39(1): 54–64. doi: 10.1016/j.cemconres.2008.09.004

55. Xu S, Simmons GC, Scherer GW. Thermal Expansion and Viscosity of Confined Liquids. *MRS Proceedings* 2003; 790: P6.8. doi: 10.1557/PROC-790-P6.8

56. Havner KS, Singh C, Varadarajan R. Plastic deformation and latent strain energy in a polycrystalline aluminum model. *International Journal of Solids and Structures* 1974; 10(8): 853–862. doi: 10.1016/0020-7683(74)90028-6

57. Halphen, B. and Nguyen Q. Sur les matériaux standard généralisés. *Journal de Mécanique* 1975; 14: 39–63.

58. Dafalias YF, Popov EP. A model of nonlinearly hardening materials for complex loading. *Acta Mechanica* 1975; 21(3): 173–192. doi: 10.1007/BF01181053

59. Coussy O. *Mechanics of Porous Continua*. England: John Wiley & Sons Ltd . 1995.

TABLE 1 Reference parameters for Boom and Opalinus clays.

Parameters		Units	Boom clay		Opalinus claystone	
			Value	Source	Value	Source
Fluid	ρ_f	kg.m^{-3}	1000	NIST ambient state	1000	NIST ambient state
	K_f	MPa	2220	NIST ambient state	2220	NIST ambient state
	α_f	K^{-1}	$2.6 \cdot 10^{-4}$	calibrated	$2.6 \cdot 10^{-4}$	calibrated
	c_f^p	J.kg^{-1}.K^{-1}	4182	NIST ambient state	4182	NIST ambient state
Porous solid	ρ_s	kg.m^{-3}	2700	Baldi [50]	2700	Horseman [43]
	κ^e	-	0.046	Picard [10]	0.008	Wileveau [45]
	G	MPa	77	Picard [10]	1500	Wileveau [45]
	α	K^{-1}	10^{-5}	Picard [10]	$1.6 \cdot 10^{-5}$	calibrated
	c_s	J.kg^{-1}.K^{-1}	1000	Baldi [50]	800	Wileveau [45]
	ϕ'	deg	23	Picard [10]	24	Wileveau [45]
	κ^p	-	0.175	Picard [10]	0.021	Wileveau [45]
	α_p	K^{-1}	10^{-4}	Picard [10]	10^{-4}	Monfared [2]
			$2 \cdot 10^{-4}$ [Fig.3(left)]	calibrated		
	a	-	$1 \cdot 10^4$	calibrated	$1 \cdot 10^4$	calibrated
	β_0	-	1.5	calibrated	3.0	calibrated
			2.4 [Fig.6]	calibrated		

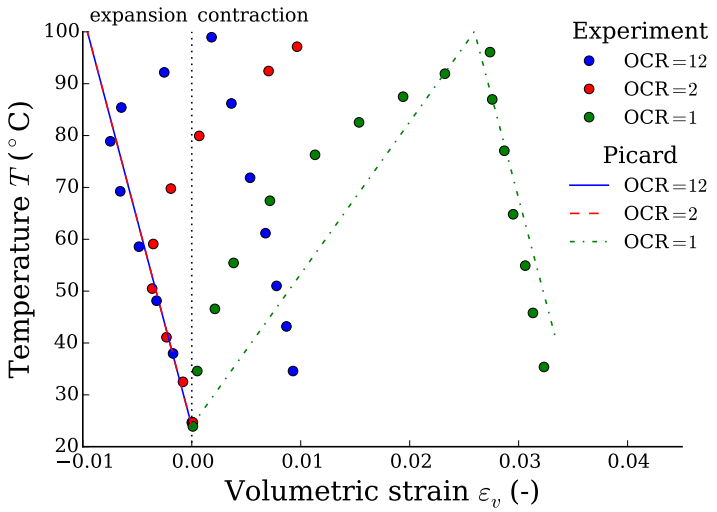

FIGURE 1 Measured and predicted volumetric strains on samples of Boom clay at three different overconsolidation ratios. Comparison between the experimental results of Sultan[24] and the predictions of Picard's model[10]. Picard's model fails at capturing the transition from reversible expansion to irreversible contraction in over-consolidated cases.

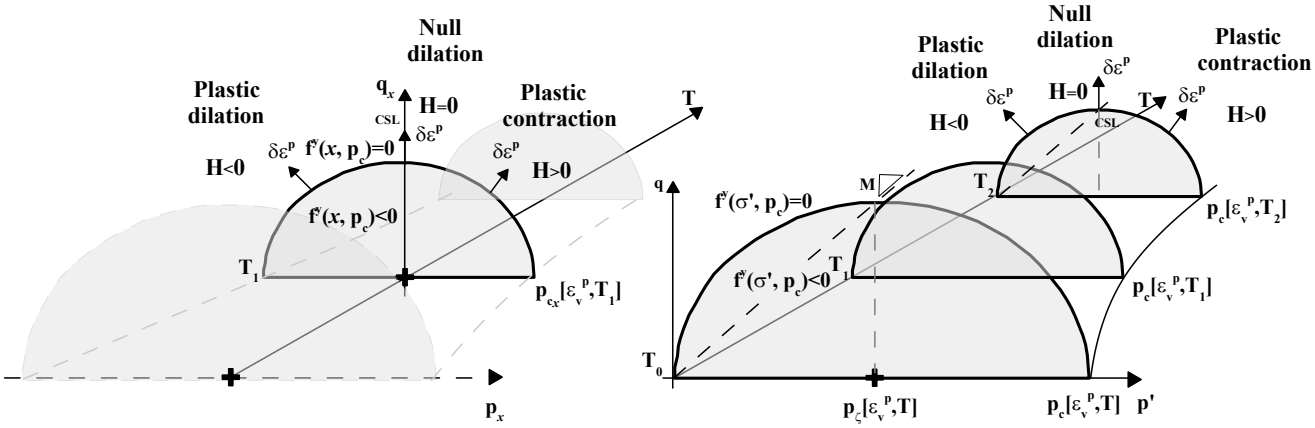

FIGURE 2 Main characteristics of the thermomechanical model with kinematic hardening of Ziegler type: (Right) Ellipsoidal loading surface in true stress space $p' - q$, with a CSL of slope M and plastic modulus H, (Left) Ellipsoidal loading surface in thermodynamic stress space $p_x - q_x$, shifted by the back stress p_ζ from the true space to the origin of coordinates in the thermodynammic space.

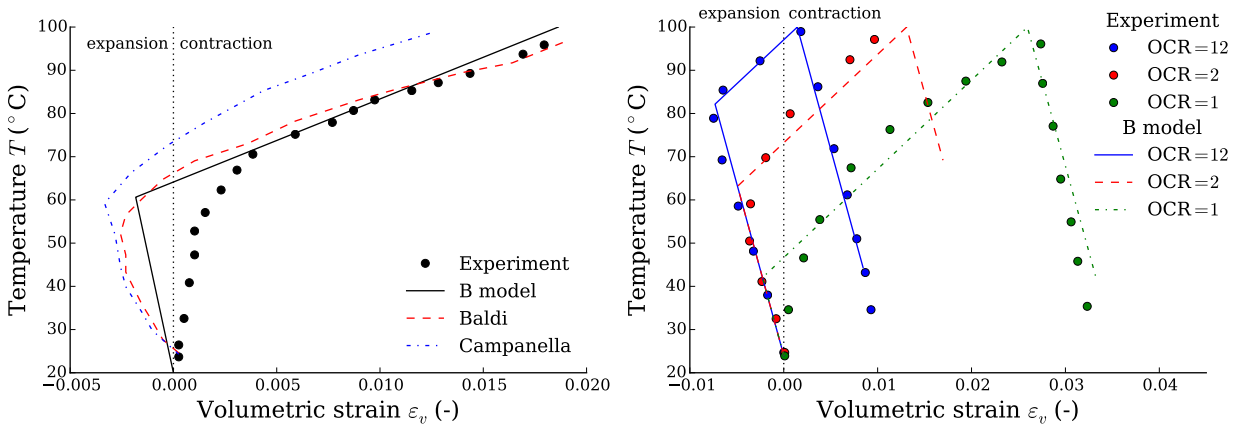

FIGURE 3 Predicted and measured volumetric strains on samples of Boom clay submitted to drained heating tests. (left) Heating tests of Delage et al.[4] (Experimental data). We report the prediction of our model, as well as the predictions of the models of Campanella[38] and Baldi[44]. (right) Heating tests of Sultan et al.[24] showing the effect of over-consolidation ratio (OCR). Combining the enhanced blocked energy with bounding plasticity makes our model able to capture accurately the behavior at different OCR.

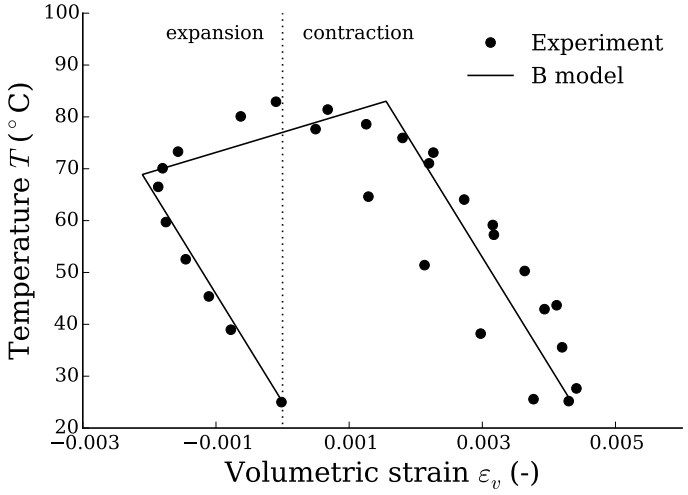

FIGURE 4 Volumetric strains during drained heating tests of Opalinus clay samples from Monfared et al.[2] compared to the prediction of the proposed model ("B model").

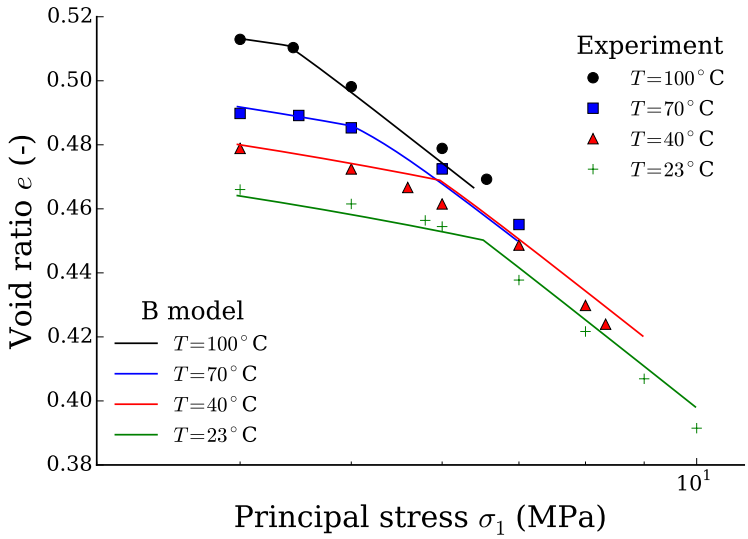

FIGURE 5 Drained oedometer tests of Boom clay performed at different temperatures[24]. Samples are initially loaded to normal consolidation (4 MPa), heated up to 100°C and, three of them, cooled down to 70°C, 40°C, and 23°C, respectively. An oedemeter test is performed on each sample, and here are reported the results of the oedometer test. One readily observes the effect of temperature on the pre-consolidation pressure. The proposed model captures well this phenomenon.

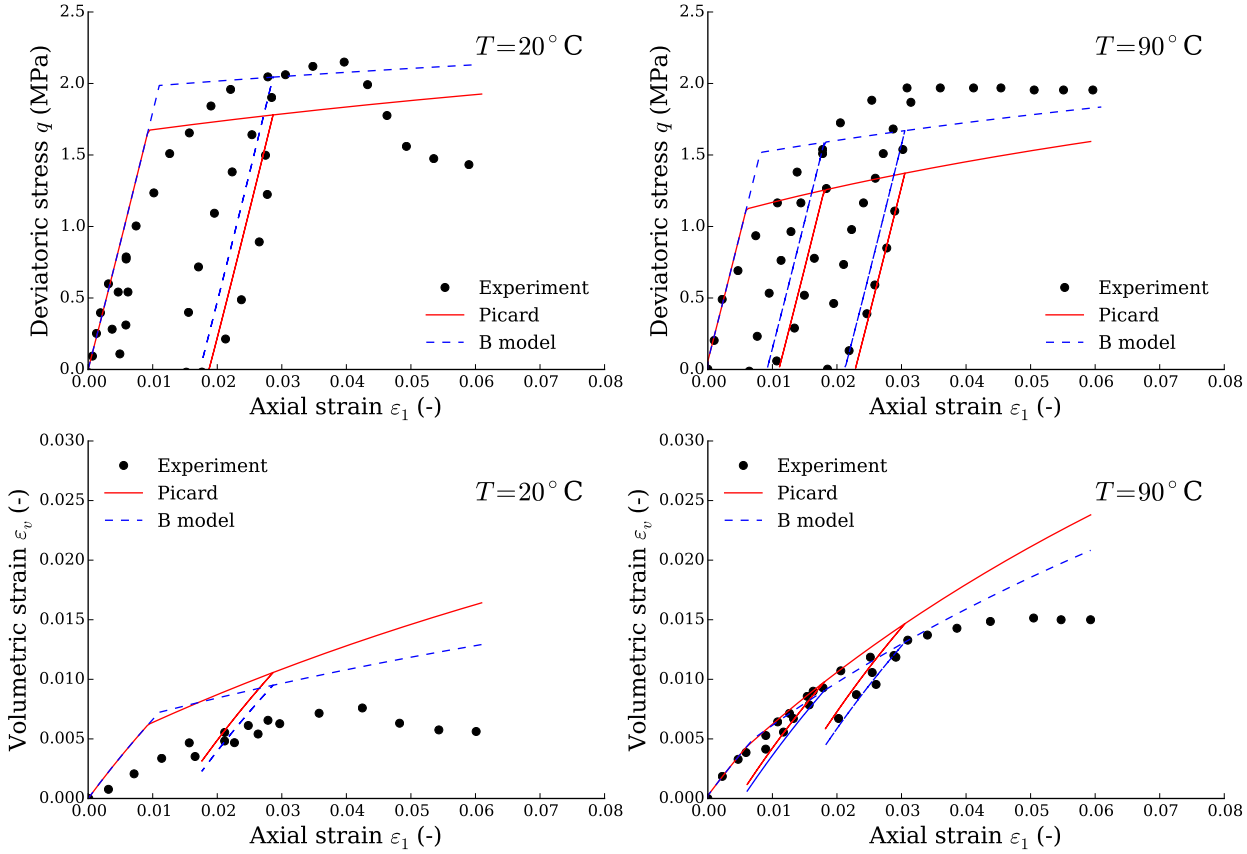

FIGURE 6 Drained triaxial tests of Boom clay reported by Baldi et al.[39] at two different temperatures: (left) 20°C and (right) 90°C. The experimental results are compared to the predictions of the proposed model, without and with bounding. (top) Stress-strain response under loading-unloading cycles. (bottom) Volumetric strains measured for the same cycles. The predictions are reasonably consistent with the experimental results regarding the stress-strain response, and the model with bounding plasticity provides more accurate results than the model without bounding plasticity. The predictions tend to over-estimate the experimental volumetric strains. This is to be attributed to an excessive Poisson's ratio, possibly due to anisotropy or to a lower bulk modulus for these samples of Boom clay, and to the non linearity of the shear modulus G at large strains.

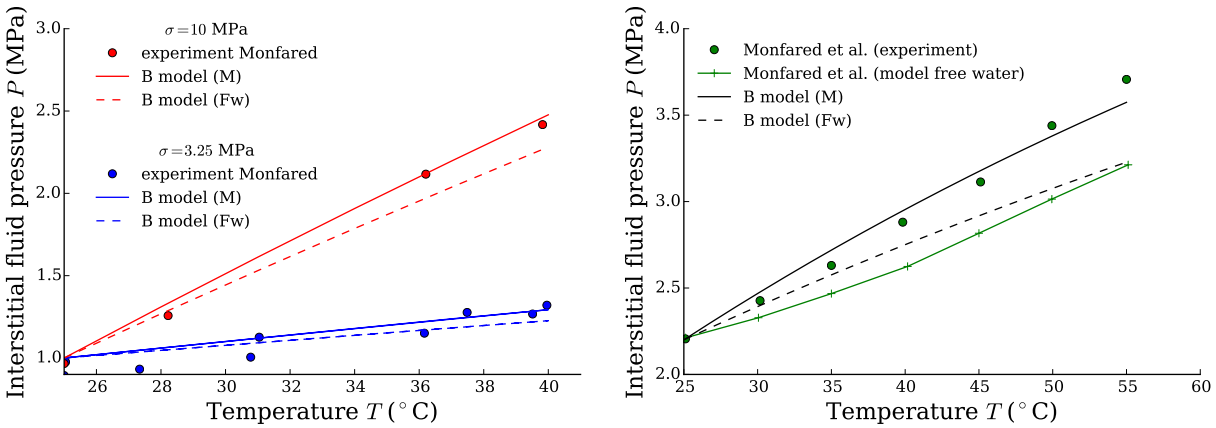

FIGURE 7 Undrained heating test on Boom clay (left) and Opalinus claystone (right) (experimental data from Monfared[3] for Boom and Monfared et al.[2] for Opalinus). Temperature is increased while the total pressure is held constant and the drainage of the water is prevented. The thermal pressurization of the fluid is measured. Poromechanical analysis under-estimate the observed pressurization, which is attributed to the anomalous behavior of adsorbed water. One can correctly predict the pressurization by considering a modified water thermal expansion (M) higher than that of free water (Fw). For Boom clay, the two experiments correspond to samples at two different total pressures and same over consolidation ratio (OCR=1.8)

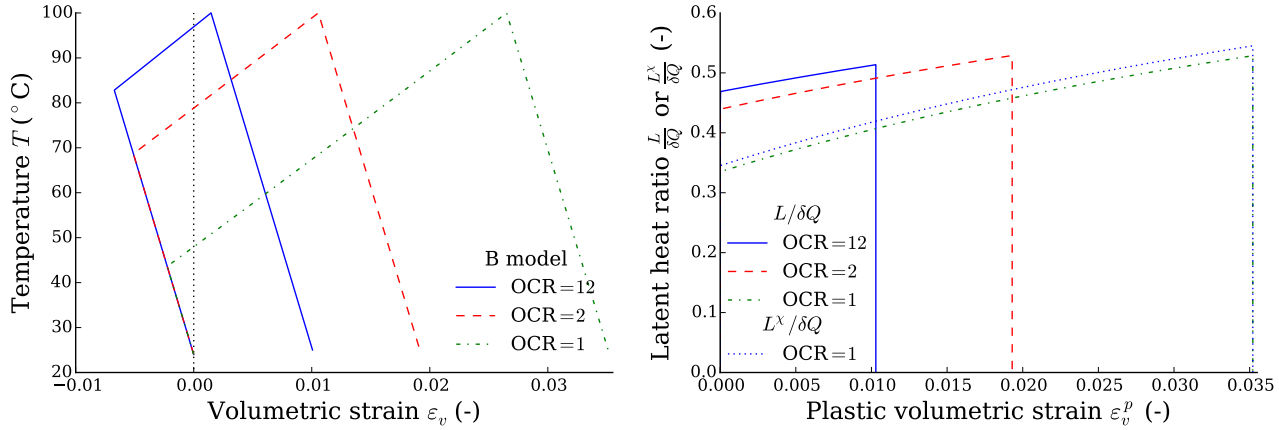

FIGURE 8 Isotropic heating tests in samples of Boom clay with different overcosolidation ratios: (a) volumteric strain vs. temperature during the heating (b) Percentage of work which remains latent in Boom clay samples during the plastic yielding stage of the isotropic heating.

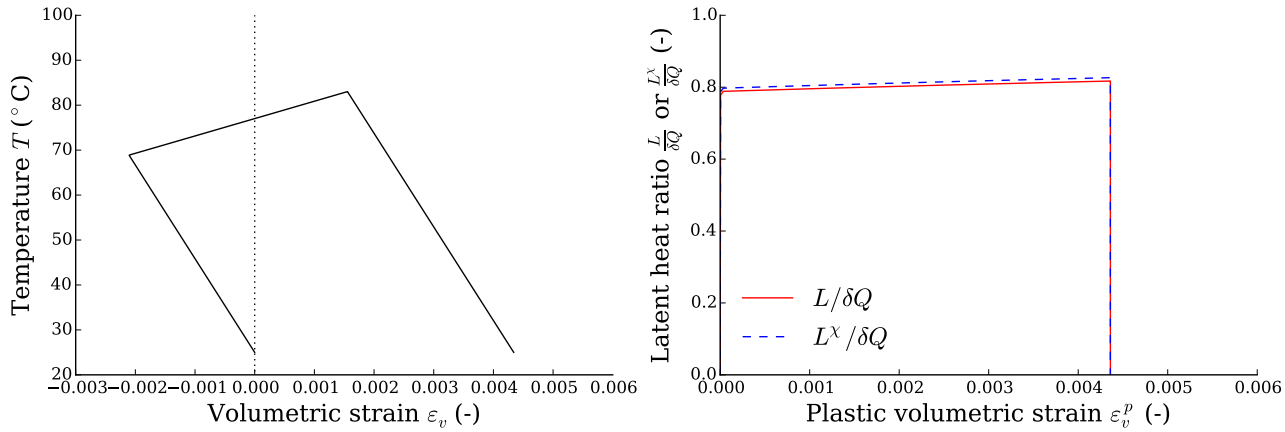

FIGURE 9 Isotropic heating-cooling test in a sample of Opalinus clay: (a) volumteric strain vs. temperature during the heating (b) Percentage of work which remains latent in Boom clay samples during the plastic yielding stage of the isotropic heating.

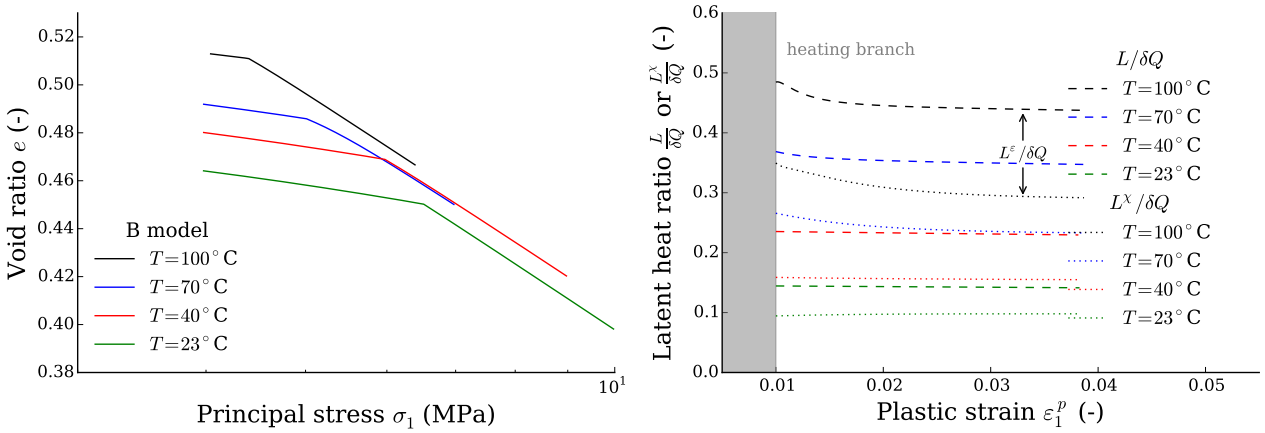

FIGURE 10 Drained oedometer tests in samples of Boom clay loaded at different temperatures: (a) void ratio vs. axial strain during the drained oedometer test for samples heated up to T=100°C, cooled down to T=70°C, T=40°C and T=23°C, (b) Percentage of work which remains latent in Boom clay samples during oedometer plastic yielding.

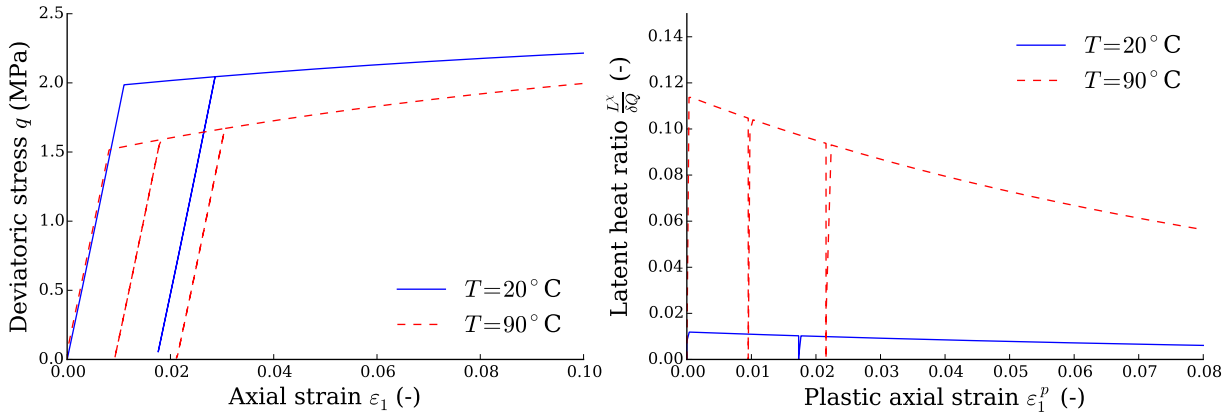

FIGURE 11 Drained triaxial test in samples of Boom clay at room temperature and at 90°C: (left) Deviatoric stress vs. axial strain during the drained triaxial for samples at room temperature and at 90°, (right) Percentage of work which remains latent in Boom clay samples during triaxial plastic yielding.

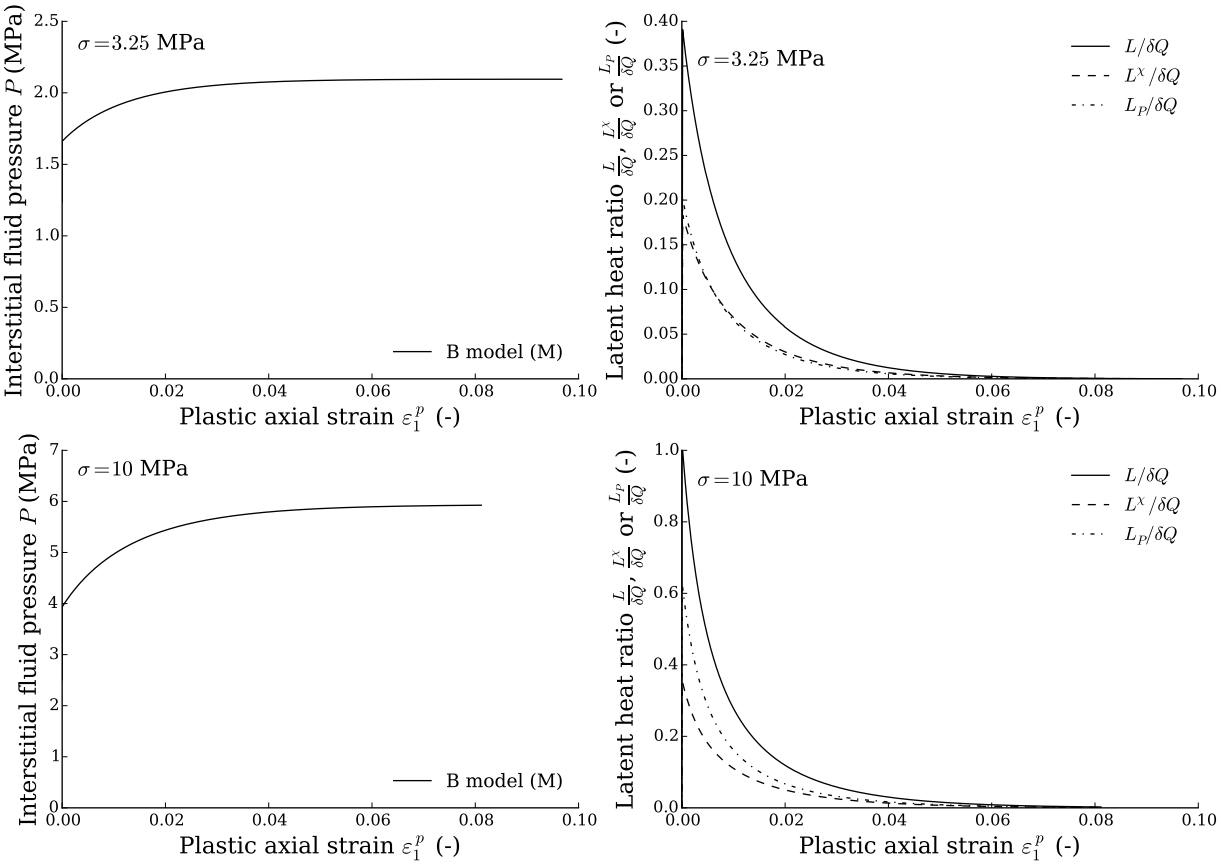

FIGURE 12 Undrained heating-triaxial test on Boom clay samples: (left) Pore pressure vs. axial plastic strain during triaxial loading, (right) Percentage of work which remain latent in Boom samples during triaxial plastic yielding. The initial state before triaxial loading results from the undrained heating test at constant total pressures of 3.25 MPa (top) and 10 MPa (bottom)

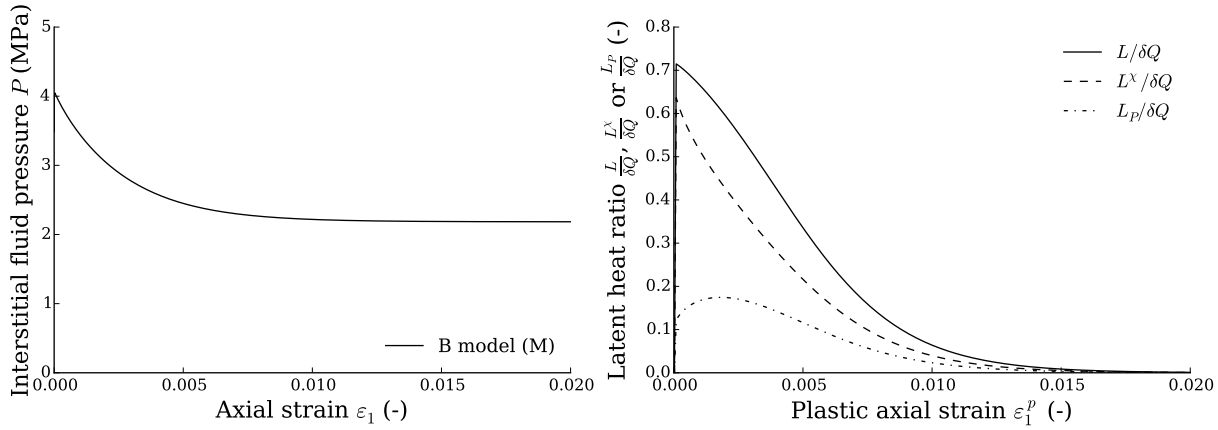

FIGURE 13 Undrained heating-triaxial test on Opalinus claystone sample: (left) Pore pressure vs. axial plastic strain during triaxial loading, (right) Percentage of work which remain latent in Opalinus sample during triaxial plastic yielding.

APPENDIX

A FIELD EQUATIONS

Modeling the behavior of the porous medium requires expressing the conservation laws that will govern the response of the open continuum. They are, the mass conservation law, the laws of thermodynamics and the generalized Newton's third law (momentum balance) for the open continuum. In this section we will develop each of these laws with the purpose of obtaining an accurate description of the field equations for the Thermo-Hydro-Mechanical porous continuum (i.e. to identify the latent energy terms of the saturated porous medium). During the development we will use terms such as "material derivative of a volume integral" or "particulate derivative of a volume integral". Terms coined by Coussy (Coussy 1991) to define: (a) the variation from t to $t + dt$ of a physical quantity attached to the whole matter and (b) the time derivative of a physical quantity when following the elementary volume Ω_t from the movement of one of the phases (fluid or skeleton), respectively. Although this work is constrained to small strain conditions, it will be necessary to start without constraining ourselves to this condition due to two main reasons: (a) the interaction between the phases that compose the porous continuum and (b) the mechanisms of dissipation that take place in this continuum which include a mechanism due to the fluid fluxes in the porous space and a mechanism due to the rate of change of internal variables in the porous solid.

Let's start by stating the mass conservation law of the open continuum. The volumetric mass density of the open continuum ρ^s is an extensive quantity and as such it can be written as a weighted sum of each individual density $\rho^s = \rho_s(1-\phi) + \phi\rho_f$ where ϕ is the porosity, ρ_s is the solid density and ρ_f is the fluid density. Furthermore, the terms $\rho = \rho_s(1-\phi)$ and $m_f = \phi\rho_f$ are known as the dry density and the wet density respectively and we will refer to them as such from now on. The mass conservation of the open continuum can be expressed as the material derivative of the volume integral of ρ^s as $\frac{D}{Dt}\int_{\Omega_t} \rho^s d\Omega_t = 0$. Owing to the mentioned extensive property of ρ^s the mass conservation law of the open system is respected if the conservation of mass of each phase is met independently. Thus, the mass conservation law of each phase can be written as

$$
\begin{aligned}
0 = \frac{d}{dt}\int_{\Omega_t} m_f d\Omega_t = \int_{\Omega_t}\left(\frac{\partial\left(\phi\rho_f\right)}{\partial t} + \operatorname{div}\left(\phi\rho_f \otimes v_i\right)\right) d\Omega_t + \int_{\Gamma_t} \underbrace{\rho_f\phi\left(v_{f_i} - v_i\right)}_{q'_{f_i}} n_i d\Gamma_t \\
0 = \frac{d}{dt}\int_{\Omega_t} \rho d\Omega_t = \int_{\Omega_t}\left(\frac{\partial\left(\rho_s(1-\phi)\right)}{\partial t} + \operatorname{div}\left(\rho_s(1-\phi)\otimes v_i\right)\right) d\Omega_t
\end{aligned}
\tag{A1}
$$

where $\frac{d}{dt}$ is the particulate derivative of a volume integral with respect to the skeleton. Notice that the convective term $\rho_f\phi\left(v_{f_i} - v_i\right)$ in Eq.A1a for the mass balance of the fluid is a consequence of considering the particle derivative of the volume integral of the wet density with respect to a frame attached to the skeleton. The local form of Eqs.A1 is obtained by using the Gauss theorem, the property $\operatorname{div}\left(x \bigotimes y\right) = x_{,i}y + xy_{,i}$ of the divergence operator and the fact that the elementary volume Ω_t is arbitrary,

$$
\begin{aligned}
0 = \rho\frac{d\vartheta_f}{dt} + q'_{f_{i,i}} = \frac{\phi}{\rho_f}\frac{d\rho_f}{dt} + \frac{d\phi}{dt} + \phi v_{i,i} + \frac{\rho_{f_i}}{\rho_f}q_{f_i} + q_{f_{i,i}} \\
0 = \frac{d\rho}{dt} + \rho v_{i,i} = \frac{(1-\phi)}{\rho_s}\frac{d\rho_s}{dt} - \frac{d\phi}{dt} + (1-\phi)\, v_{i,i}
\end{aligned}
\tag{A2}
$$

By adding together Eqs.A2, the combined continuity equation of the porous continuum is obtained

$$
0 = v_{i,i} + q_{f_{i,i}} + \frac{\rho_{f,i}}{\rho_f}q_{f_i} + \frac{\phi}{\rho_f}\frac{d\rho_f}{dt} - (1-\phi)\, v^s_{i,i} \tag{A3}
$$

where the density of the solid has been expressed in terms of the volume $\mathrm{v_s}$ and the identity $\frac{1}{v_s}\frac{dv_s}{dt} = \operatorname{div}\left(v^s_i\right)$ has been used. With this result available, let's proceed with the laws of thermodynamics. Based on the postulate of local state, the total energy

balance in the porous continuum (first law of thermodynamics) states that the rate of increase of kinetic energy K and internal energy e in the porous volume Ω_t is equal to the power input to the volume L given by the energy input at the boundary Γ_t and the rate of work of body forces. Assuming thermal equilibrium between the phases (equal temperature) of the porous continuum the first law of thermodynamics is stated as,

$$\frac{DK}{Dt} + \frac{D}{Dt}\int_{\Omega_t} \rho e d\Omega_t = \int_{\Omega_t} L d\Omega_t - \int_{\Gamma_t} q_{h_i} n_i d\Gamma_t \tag{A4}$$

where $\vec{q}_h$ is the convective heat flux entering to the porous volume and $\frac{D}{Dt}(\bullet)$ denotes the variation of a quantity (e.g. kinetic energy) attached to the whole matter contained at time t in the volume Ω_t (Coussy 1991) and is defined as $\frac{D}{Dt}(\bullet) = \frac{d}{dt}(\bullet) + \frac{d^f}{dt}(\bullet)$. Kinetic energy should be considered in the energy balance if inertia terms are relevant in the momentum balance of the system. The kinetic energy of the porous continuum is an extensive quantity and as such may be written as the sum of the kinetic energy of the fluid K_f and the kinetic energy of the porous solid K_s. Thus it can be expressed in terms of the absolute solid and fluid velocities, the dry and wet densities, as $K = K_s + K_f = \int_{\Omega_t} \left(\rho \frac{v_i v_i}{2} + m_f \frac{v_{f_i} v_{f_i}}{2}\right) d\Omega_t$.

Using the particle derivative of a volume integral, the rate of change of kinetic energy in the volume Ω_t can be expressed as,

$$\frac{DK}{Dt} = \int_{\Omega_t} \frac{\partial}{\partial t}\left(m_f \frac{v_{f_i} v_{f_i}}{2} + \rho \frac{v_i v_i}{2}\right) d\Omega_t + \int_{\Gamma_t} \left(m_f \frac{v_{f_i} v_{f_i}}{2}\right) v_{f_i} n_i d\Gamma_t + \int_{\Gamma_t} \left(\rho \frac{v_i v_i}{2}\right) v_i n_i d\Gamma_t \tag{A5}$$

The first term in Eq.A5 represents the stored kinetic energy which changes with time while the second and the third terms account for the net flows of kinetic energy through the element boundary due to the fluid and the porous solid respectively. Using the Gauss theorem Eq.A5 can be expanded as

$$\begin{aligned} \frac{DK}{Dt} = &\int_{\Omega_t} m_f v_{f_i} \underbrace{\left(\frac{\partial v_{f_i}}{\partial t} + v_{f_{i,i}} v_{f_i}\right)}_{a_{f_i}} d\Omega_t + \int_{\Omega_t} \rho v_i \underbrace{\left(\frac{\partial v_i}{\partial t} + v_{i,i} v_i\right)}_{a_i} d\Omega_t + \int_{\Omega_t} \underbrace{\left(\frac{\partial \rho}{\partial t} + \operatorname{div}\left(\rho \otimes v_i\right)\right)}_{=0} \frac{v_i v_i}{2} d\Omega_t \\ &+ \int_{\Omega_t} \underbrace{\left(\frac{\partial m_f}{\partial t} + \operatorname{div}\left(m_f \otimes v_i\right) + q'_{f_{i,i}}\right)}_{=0} \frac{v_{f_i} v_{f_i}}{2} d\Omega_t \end{aligned} \tag{A6}$$

The third and fourth terms in Eq.A6 vanished due to the fluid (Eq. A1a) and solid (Eq. A1b) mass conservations, while the first two terms introduces the definition of acceleration for a fluid particle $\vec{a}_f$ and for a solid particle $\vec{a}$.

The overall specific internal energy e in Eq.A4 is an extensive quantity and as such it can be expressed as a weighted sum of the specific internal energy in the fluid $e_f = \frac{E_f}{M_f}$ and the specific internal energy in the porous solid $e_s = \frac{E_s}{M_s}$ such that $e = e_s + \vartheta_f \frac{E_f}{M_f}$ (Coussy 2004, Eq. 316) where $\vartheta_f = \frac{m_f}{\rho}$ is the ratio between the wet and the dry densities. Thus the rate of change of internal energy in a material volume Ω_t of a porous continuum is expressed as,

$$\frac{D}{Dt}\int_{\Omega_t} \rho \left(e_s + \vartheta_f \frac{E_f}{M_f}\right) d\Omega_t = \frac{d}{dt}\int_{\Omega_t} \left(\rho e_s + m_f e_f\right) d\Omega_t + \int_{\Gamma_t} j'_{e_{f_i}} n_i d\Gamma_t \tag{A7}$$

where $\vec{j}'_{e_f} = \frac{E_f}{M_f}\vec{q}'_f$ is the spatial description of the energy flux in the fluid due to its relative motion with respect to the porous solid.

Finally, the rate of work input L (in Eq.A4) to a saturated porous material is defined in an Eulerian description by the work rate due to the traction forces $\vec{t}_i^f$ acting on the fluid boundary $\phi\Gamma_t$ and the traction forces $\vec{t}_i^{sk}$ (forces per unit area) acting on the boundary of the porous solid $(1-\phi)\Gamma_t$, such that $\vec{t}_i = \vec{t}_i^{sk} + \vec{t}_i^f$. Then the Eulerian expression for the work rate of the traction forces is $\vec{t}_i^{sk} v_i + \vec{t}_i^f v_{f_i} = (1-\phi)\sigma_{ij}^s n_j v_j - \phi P n_i v_{f_{I_i}} = \sigma_{ij} n_j v_i - P q_{f_i} n_i$ where n_i is the unit normal to Γ_t at $\vec{x}$, σ_{ij}^s is the average

stress tensor acting in the solid and $P\delta_{ij}\left(\equiv\sigma_{ij}^{f}\right)$ is the average stress tensor acting in the fluid. Thus, the power input to the saturated porous continuum is,

$$\int_{\Omega_t} L d\Omega_t = \int_{\Gamma_t} \left(\sigma_{ij} n_j v_i - P q_{f_i} n_i\right) d\Gamma_t + \int_{\Omega_t} \left(\rho v_i + m_f v_{f_i}\right) g_i d\Omega_t \tag{A8}$$

Combining equations A4-A8 the expanded integral form of the energy balance (Eq. A4) for the saturated porous continuum is expressed as,

$$\begin{aligned} &\int_{\Omega_t} \rho\left(a_i + \vartheta_f a_{f_i}\right) v_i d\Omega_t + \int_{\Omega_t} q'_{f_i} a_{f_i} d\Omega_t + \frac{d}{dt}\int_{\Omega_t}\left(\rho e_s + \vartheta_f \frac{E_f}{M_f}\right) d\Omega_t + \int_{\Gamma_t} j'_{e_{f_i}} n_i d\Gamma_t = \\ &\int_{\Gamma_t}\left(\sigma_{ij} n_j v_i - P q_{f_i} n_i\right) d\Gamma_t + \int_{\Omega_t}\left(\rho v_i + m_f v_{f_i}\right) g_i d\Omega_t - \int_{\Gamma_t} q_{h_i} n_i d\Gamma_t \end{aligned} \tag{A9}$$

Applying the divergence theorem of Gauss and due to the arbitrariness of the current porous volume Ω_t, the local form of Eq.A9 is,

$$\begin{aligned} &\rho\left(\frac{de_s}{dt} + \vartheta_f \frac{de_f}{dt}\right) + \left(\frac{E_f}{M_f}\right)_{,i} = \left(\sigma_{ij,j} + \rho\left(\left(g_i - a_i\right) + \vartheta_f g_i\right) - m_f a_{f_i}\right) v_i \\ &+\sigma_{ij} v_{i,j}^{sym} + \sigma_{ij}\omega_{ij} + \left(\rho_f\left(g_i - a_{f_i}\right) - P_{,i}\right) q_{f_i} - P q_{f_{i,i}} - q_{h_{i,i}} \end{aligned} \tag{A10}$$

where the divergence of the solid velocity $v_{i,j}$ has been split into its symmetric $v_{i,j}^{sym} = \frac{1}{2}\left(v_{i,j} + v_{j,i}\right)$ and non-symmetric $\omega_{ij} = \frac{1}{2}\left(v_{i,j} - v_{j,i}\right)$ parts. The terms $\left(\sigma_{ij,j} + \rho\left(\left(g_i - a_i\right) + \vartheta_f g_i\right) - m_f a_{f_i}\right) v_i$ and $\sigma_{ij}\omega_{ij}$ represents rigid movements[59,51] and as such, they do not contribute to the change of the overall specific internal energy, as a consequence they can be dropped from Eq.A10. Moreover the expression between brackets in the first of these terms is the generalized Newton's third law (momentum balance)

$$0 = \sigma_{ij,j} + \rho\left(\left(g_i - a_i\right) + \vartheta_f g_i\right) - m_f a_{f_i} \tag{A11}$$

Notice that the divergence of the Cauchy stress tensor is taken with respect to the position in the current configuration which evidences an Eulerian approach for the porous solid. In field conditions, the fluid and the solid phases are exchanging energy and volume (porosity) so that the two phases are in thermal and mechanical equilibrium and share the same temperature T and pore pressure P. The thermodynamic potential minimum in such conditions is not the overall specific internal energy e but the Legendre transform corresponding to the sum of Gibbs free enthalpy of the fluid g_f and the Helmholtz free energy of the solid f_s. This transformation interchanges the roles of the overall specific entropy s and the porosity ϕ with the temperature T and the fluid pressure P respectively, such that $e_s + \vartheta_f \frac{E_f}{M_f} = f_s + \vartheta_f \frac{G_f}{M_f} + T s_s + \frac{\vartheta_f}{M_f}\left(T S_f - P\frac{M_f}{\rho_f}\right)$. Thus the rate of change of the internal energy in the porous continuum can be expressed as,

$$\rho\left(\frac{de_s}{dt} + \vartheta_f \frac{de_f}{dt}\right) = \rho\left(\frac{df_s}{dt} + \vartheta_f \frac{dg_f}{dt}\right) + \rho\left(s_s + \vartheta_f \frac{S_f}{M_f}\right)\frac{dT}{dt} + \rho T\left(\frac{ds_s}{dt} + \vartheta_f \frac{ds_f}{dt}\right) - \phi\frac{dP}{dt} + \frac{\phi}{\rho_f} P \frac{d\rho_f}{dt} \tag{A12}$$

Combining Eq.A3, Eq.A10 and Eq.A12 is possible to obtain an expression for the total energy balance in the porous continuum in terms of f_s and g_f,

$$\begin{aligned} &\rho\left(\frac{df_s}{dt} + \vartheta_f \frac{dg_f}{dt}\right) + \rho\left(s_s + \vartheta_f \frac{S_f}{M_f}\right)\frac{dT}{dt} + \rho T\left(\frac{ds_s}{dt} + \vartheta_f \frac{ds_f}{dt}\right) - \phi\frac{dP}{dt} = \left(\sigma_{ij} + P\delta_{ij}\right) v_{i,j}^{sym} \\ &-(1-\phi) P v_{i,i}^{s} + \left(\rho_f\left(g_i - a_{f_i}\right) - P_{,i}\right) q_{f_i} - q_{h_{i,i}} - \left(\left(\frac{E_f}{M_f}\right)_{,i} - P\frac{\rho_{f,i}}{\rho_f^2}\right) q'_{f_i} \end{aligned} \tag{A13}$$

If small strains are assumed to develop the material and the spatial coordinates coincide and as consequence the small strain tensor describe the deformation of the porous medium and $\rho = \rho_0$ the initial dry density. If the solid matrix is

TABLE A1 Primary state equations for the porous continuum

Description	State Equation	No. of Eqs.
Effective stress in Biot's scense	$\sigma_{ij}^{'} = \rho_0 \left.\frac{\partial f_s}{\partial \varepsilon_{ij}}\right\|_{T,\varepsilon_{ij}^p,\chi_{ij}}$	6
Entropy in the solid	$-s_s = \left.\frac{\partial f_s}{\partial T}\right\|_{\varepsilon_{ij},\varepsilon_{ij}^p,\chi_{ij}}$	1
Porosity	$\phi = m_f \left.\frac{\partial g_f}{\partial P}\right\|_T$	1
Entropy in the fluid	$-s_f = \left.\frac{\partial g_f}{\partial T}\right\|_P$	1

assumed incompressible $\left(v_i^s = 0\right)$ the following dependency for the Helmholtz energy function of the solid can be accepted $f_s\left(\varepsilon_{ij}, T, \varepsilon_{ij}^p, \chi_{ij}\right) \equiv f_e\left(\varepsilon_{ij} - \frac{\varepsilon_{ij}^p + \chi_{ij}}{2}, T\right) + V\left(T, \chi_{ij}\right)$ and for the Gibbs free enthalpy of the fluid $g_f\left(P, T\right)$ such that,

$$\frac{df_s}{dt} = \left.\frac{\partial f_e}{\partial \varepsilon_{ij}}\right|_T \left(\dot{\varepsilon}_{ij} - \frac{\dot{\varepsilon}_{ij}^p + \dot{\chi}_{ij}}{2}\right) + \left.\frac{\partial f_s}{\partial T}\right|_{\varepsilon_{ij},\varepsilon_{ij}^p,\chi_{ij}} \frac{\partial T}{\partial t} + \left.\frac{-\partial V}{\partial \chi_{ij}}\right|_T \dot{\chi}_{ij}$$
$$\frac{dg_f}{dt} = \left.\frac{\partial g_f}{\partial P}\right|_T \frac{\partial P}{\partial t} + \left.\frac{\partial g_f}{\partial T}\right|_P \frac{\partial T}{\partial t} \tag{A14}$$

Combining Eq.A13 and Eq.A14 we obtain,

$$\rho_0 T\left(\frac{\partial s_s}{\partial t} + \vartheta_f \frac{\partial s_f}{\partial t}\right) = \left(\sigma_{ij}^{'} - \rho_0 \left.\frac{\partial f_e}{\partial \varepsilon_{ij}}\right|_{T,\varepsilon_{ij}^p,\chi_{ij}}\right)\dot{\varepsilon}_{ij} + \rho_0 \left.\frac{\partial f_e}{\partial \varepsilon_{ij}}\right|_{T,\varepsilon_{ij}^p,\chi_{ij}} \left(\frac{\dot{\varepsilon}_{ij}^p + \dot{\chi}_{ij}}{2}\right) +$$
$$-\rho_0 \left(s_s + \left.\frac{\partial f_s}{\partial T}\right|_{\varepsilon_{ij},\varepsilon_{ij}^p,\chi_{ij}}\right)\frac{\partial T}{\partial t} - \rho_0 \left.\frac{-\partial V}{\partial \chi_{ij}}\right|_T \dot{\chi}_{ij} +$$
$$\left(\phi - m_f \left.\frac{\partial g_f}{\partial P}\right|_T\right)\frac{\partial P}{\partial t} - m_f \left(s_f + \left.\frac{\partial g_f}{\partial T}\right|_P\right)\frac{\partial T}{\partial t} + \left(\rho_f\left(g_i - a_{f_i}\right) - P_{,i}\right) q_{f_i} - q_{h_{i,i}} -$$
$$\left(\left(\frac{E_f}{M_f}\right)_{,i} - P\frac{\rho_{f,i}}{\rho_f^2}\right) q_{f_i}^{'} \tag{A15}$$

where $\sigma_{ij}^{'} = \sigma_{ij} + P\delta_{ij}$ is the effective stress tensor. Equation A15 must be satisfied for any value of $\frac{\partial T}{\partial t}$, $\frac{\partial P}{\partial t}$, $\dot{\varepsilon}_{ij}$, since they are independent variables, leading to the set of primary state equations, TableA1.
Then Eq.A15 simplifies to,

$$\rho_0 T\left(\frac{\partial s_s}{\partial t} + \vartheta_f \frac{\partial s_f}{\partial t}\right) = \sigma_{ij}^{'}\left(\frac{\dot{\varepsilon}_{ij}^p + \dot{\chi}_{ij}}{2}\right) - \rho_0 \left.\frac{-\partial V}{\partial \chi_{ij}}\right|_T \dot{\chi}_{ij} + \left(\rho_f\left(g_i - a_{f_i}\right) - P_{,i}\right) q_{f_i}$$
$$-q_{h_{i,i}} - \left(\left(\frac{E_f}{M_f}\right)_{,i} - P\frac{\rho_{f,i}}{\rho_f^2}\right) q_{f_i}^{'} \tag{A16}$$

Due to the state equations for the entropy in the solid and for the entropy in the fluid, let the entropy in the porous continuum be $s = s_s + \vartheta_f \frac{S_f}{M_f}$ such that $s_s = s_e\left(\varepsilon_{ij} - \frac{\varepsilon^p_{ij}+\chi_{ij}}{2}, T\right) + s^b_s\left(T, \chi_{ij}\right)$ and $s_f\left(P, T\right)$. Then,

$$\frac{\partial s_s}{\partial t} = \left.\frac{\partial s_e}{\partial \varepsilon_{ij}}\right|_{\phi,T,\varepsilon^p_{ij},\chi_{ij}} \left(\dot{\varepsilon}_{ij} - \frac{\dot{\varepsilon}^p_{ij} + \dot{\chi}_{ij}}{2}\right) + \left.\frac{\partial s_s}{\partial T}\right|_{\varepsilon_{ij},\varepsilon^p_{ij},\chi_{ij}} \frac{\partial T}{\partial t} + \left.\frac{-\partial s^b_s}{\partial \chi_{ij}}\right|_T \dot{\chi}_{ij}$$
$$\frac{\partial s_f}{\partial t} = \left.\frac{\partial s_f}{\partial P}\right|_T \frac{\partial P}{\partial t} + \left.\frac{\partial s_f}{\partial T}\right|_P \frac{\partial T}{\partial t} \tag{A17}$$

Combining Eq.A16 and Eq.A17, considering the primary state equations summarized in Tab.A1 and due to the known definitions $\frac{\partial s_s}{\partial T} = \frac{c_s}{T}$ and $\frac{\partial s_f}{\partial T} = \frac{c^p_f}{T}$ the temperature field equation of the porous continuum is,

$$c_p \frac{\partial T}{\partial t} = -m_f T \left.\frac{-\partial\left(\frac{\phi}{m_f}\right)}{\partial T}\right|_T \frac{\partial P}{\partial t} - \rho_0 T \left.\frac{-\partial\left(\frac{\sigma'_{ij}}{\rho}\right)}{\partial T}\right|_{T,\varepsilon^p_{ij},\chi_{ij}} \left(\dot{\varepsilon}_{ij} - \frac{\dot{\varepsilon}^p_{ij} + \dot{\chi}_{ij}}{2}\right) + \rho_0 T \left.\frac{-\partial\left(\frac{\partial V}{\partial \chi_{ij}}\right)}{\partial T}\right|_T \dot{\chi}_{ij} +$$
$$\sigma'_{ij}\left(\frac{\dot{\varepsilon}^p_{ij} + \dot{\chi}_{ij}}{2}\right) - \rho_0 \left.\frac{-\partial V}{\partial \chi_{ij}}\right|_T \dot{\chi}_{ij} + \left(\rho_f\left(g_i - a_{f_i}\right) - P_{,i}\right) q_{f_i} - q_{h_{i,i}} - \left(\left(\frac{E_f}{M_f}\right)_{,i} - P\frac{\rho_{f,i}}{\rho_f^2}\right) q'_{f_i} \tag{A18}$$

where $c_p = \rho_0 c_s + m_f c^p_f$ is the specific heat capacity of the porous continuum.

The dissipation terms in Eq.A18 can be understood more clearly if the second law of thermodynamic is invoked. The law that states that the quantity of energy which can be transformed into efficient mechanical work can only evolve irreversible. After having introduced the entropy of the porous continuum, the second law of thermodynamics for a subsystem of porous continuum Ω_t reads,

$$\frac{D}{Dt}\int_{\Omega_t} \rho_0 \left(s_s + \vartheta_f \frac{S_f}{M_f}\right) d\Omega_t \equiv \frac{d}{dt}\int_{\Omega_t} \rho_0 \left(s_s + \vartheta_f \frac{S_f}{M_f}\right) d\Omega_t + \int_{\Gamma_t} j'_{S_f} n_i d\Gamma_t \geq \frac{d}{dt}\int_{\Omega_t} \rho_0 \left(s^r_s + \vartheta_f \frac{S^r_f}{M_f}\right) d\Omega_t$$
$$+ \int_{\Gamma_t} j'_{S^r_f} n_i d\Gamma_t \equiv \int_{\Gamma_t} -\frac{q_{h_i} n_i}{T} d\Gamma_t \tag{A19}$$

where the relative fluxes of entropy in the fluid are $\vec{j}'_{S_f} = \frac{S_f}{M_f}\vec{q}'_f$ and $\vec{j}'_{S^r_f} = \frac{S^r_f}{M_f}\vec{q}'_f$ and the superscript $()^r$ makes reference to the reversible part of the entropy. The reversible entropy is the one supplied to the subsystem of porous continuum from its surroundings. Applying the divergence theorem of Gauss to Eq.A19 and after expanding derivatives the local form of the fundamental inequality is expressed as,

$$\rho_0 D \equiv \rho \frac{Ds^i}{Dt} = \rho_0 T\left(\frac{ds_s}{dt} + \vartheta_f \frac{ds_f}{dt}\right) + T\left(\frac{S_f}{M_f}\right)_{,i} q'_{f_i} + q_{h_{i,i}} - \frac{q_{h_i} T_{,i}}{T} \geq 0 \tag{A20}$$

Using Eq.A16 obtained after the Legendre transformation $f_s + \vartheta_f \frac{G_f}{M_f} = e - T s_s - \frac{\vartheta_f}{M_f}\left(T S_f - P\frac{M_f}{\rho_f}\right)$ the fundamental inequality is expressed in the terms of the rate of plastic strains ε^p_{ij}, the rate of internal variables χ_{ij} and the fluid flux $\vec{q}_f$,

$$\rho_0 D = \left(\rho_f\left(g_i - a_{f_i}\right) - P_{,i}\right) q_{f_i} - \rho_0 \left.\frac{\partial f_s}{\partial \varepsilon^p_{ij}}\right|_{\varepsilon_{ij},\phi,T,\chi_{ij}} \dot{\varepsilon}^p_{ij} - \rho_0 \left.\frac{\partial f_s}{\partial \chi_{ij}}\right|_{\varepsilon_{ij},\phi,T,\varepsilon^p_{ij}} \dot{\chi}_{ij} - \frac{q_{h_i} T_{,i}}{T} \geq 0 \tag{A21}$$

In order to enclose in a general formulation either mechanism of dissipation and to preserve the true potential status of the dissipation potential Halphen (1975) proposed to introduce the force potential function Z such that the dissipation is $D = \frac{\partial Z}{\partial x_i} x_i$. Let the force potential admits the following dependency $Z = Z\left(q_{f_i}, \dot{\varepsilon}^p_{ij}, \dot{\chi}_{ij}, \frac{q_{h_i}}{T}\right)$ such that,

$$\rho_0 D = \rho_0 \left.\frac{\partial Z}{\partial q_{f_i}}\right]_{\dot{\varepsilon}^p_{ij},\dot{\chi}_{ij},\frac{q_{h_i}}{T}} q_{f_i} + \rho_0 \left.\frac{\partial Z}{\partial \dot{\varepsilon}^p_{ij}}\right]_{q_{f_i},\dot{\chi}_{ij},\frac{q_{h_i}}{T}} \dot{\varepsilon}^p_{ij} + \rho_0 \left.\frac{\partial Z}{\partial \dot{\chi}_{ij}}\right]_{q_{f_i},\dot{\varepsilon}^p_{ij},\frac{q_{h_i}}{T}} \dot{\chi}_{ij} + \rho_0 \left.\frac{\partial Z}{\partial \frac{q_{h_i}}{T}}\right]_{q_{f_i},\dot{\varepsilon}^p_{ij},\dot{\chi}_{ij},\frac{q_{h_i}}{T}} \frac{q_{h_i}}{T} \tag{A22}$$

TABLE A2 Complementary state equations for the porous continuum

Description	State Equation	No. of Eqs.
Thermodynamic stress	$\tilde{x}_{ij} = \rho_0 \left.\frac{\partial Z}{\partial \dot{\varepsilon}^p_{ij}}\right\|_{q_{f_i},\dot{\chi}_{ij},\frac{q_{h_i}}{T}} = -\rho_0 \left.\frac{\partial f_s}{\partial \varepsilon^p_{ij}}\right\|_{\varepsilon_{ij},\phi,T,\chi_{ij}}$	6
Thermodynamic stress	$\hat{x}_{ij} = \rho_0 \left.\frac{\partial Z}{\partial \dot{\chi}_{ij}}\right\|_{q_{f_i},\dot{\varepsilon}^p_{ij},\frac{q_{h_i}}{T}} = -\rho_0 \left.\frac{\partial f_s}{\partial \chi_{ij}}\right\|_{\varepsilon_{ij},\phi,T,\varepsilon^p_{ij}}$	1
Thermodynamic force	$\left(\rho_f \left(g_i - a_{f_i}\right) - P_{,i}\right) = \rho_0 \left.\frac{\partial Z}{\partial q_{f_i}}\right\|_{\dot{\varepsilon}^p_{ij},\dot{\chi}_{ij},\frac{q_{h_i}}{T}}$	1
Heat conduction	$-T_{,i} = \rho_0 \left.\frac{\partial Z}{\partial \frac{q_{h_i}}{T}}\right\|_{q_{f_i},\dot{\varepsilon}^p_{ij},\dot{\chi}_{ij},\frac{q_{h_i}}{T}}$	1

Combining equations A21 and A22 we obtain

$$\left(\left(\rho_f \left(g_i - a_{f_i}\right) - P_{,i}\right) - \rho_0 \left.\frac{\partial Z}{\partial q_{f_i}}\right|_{\dot{\varepsilon}^p_{ij},\dot{\chi}_{ij},\frac{q_{h_i}}{T}}\right) q_{f_i} - \left(\rho_0 \left.\frac{\partial f_s}{\partial \varepsilon^p_{ij}}\right|_{\varepsilon_{ij},\phi,T,\chi_{ij}} + \rho_0 \left.\frac{\partial Z}{\partial \dot{\varepsilon}^p_{ij}}\right|_{q_{f_i},\dot{\chi}_{ij},\frac{q_{h_i}}{T}}\right) \dot{\varepsilon}^p_{ij} -$$
$$\left(\rho_0 \left.\frac{\partial f_s}{\partial \chi_{ij}}\right|_{\varepsilon_{ij},\phi,T,\varepsilon^p_{ij}} + \rho_0 \left.\frac{\partial Z}{\partial \dot{\chi}_{ij}}\right|_{q_{f_i},\dot{\varepsilon}^p_{ij},\frac{q_{h_i}}{T}}\right) \dot{\chi}_{ij} - \left(T_{,i} + \rho_0 \left.\frac{\partial Z}{\partial \frac{q_{h_i}}{T}}\right|_{q_{f_i},\dot{\varepsilon}^p_{ij},\dot{\chi}_{ij},\frac{q_{h_i}}{T}}\right) \frac{q_{h_i}}{T} \geq 0 \tag{A23}$$

Equation A23 must be satisfied for any value of q_{f_i}, $\dot{\varepsilon}^p_{ij}$, $\dot{\chi}_{ij}$, $\frac{q_{h_i}}{T}$, since they are independent variables. Then, the set of complementary state equations of the porous continuum is obtained, see Table A2.

Because of the layout of the Helmholtz energy function f_s, the definition of the back stress $\zeta_{ij} = \frac{-\partial V}{\partial \chi_{ij}}$ and the state equations summarized in Tab.A1 and Tab. A2, Eq.A21 can be re-written as

$$\rho_0 D = \left(\rho_f \left(g_i - a_{f_i}\right) - P_{,i}\right) q_{f_i} + \rho_0 \tilde{x}_{ij} \dot{\varepsilon}^p_{ij} + \rho_0 \underbrace{\left(\frac{\sigma'_{ij}}{2} - \zeta_{ij}\right)}_{\hat{x}_{ij}} \dot{\chi}_{ij} - \frac{q_{h_i} T_{,i}}{T} \geq 0 \tag{A24}$$

Equation A24 highlights the three dissipation mechanisms that develop in the saturated porous medium. The first term corresponds to the mechanism due to the fluid flow, the second one is due to the mechanical dissipation and the third one is the thermal dissipation. If $\varepsilon^p_{ij} = \chi_{ij}$ Eq.A24 simplifies to $\rho_0 D = \left(\rho_f \left(g_i - a_{f_i}\right) - P_{,i}\right) q_{f_i} + \rho_0 x_{ij} \dot{\varepsilon}^p_{ij} - \frac{q_{h_i} T_{,i}}{T} \geq 0$ where $\mathrm{x_{ij}} = \tilde{\mathrm{x}}_{\mathrm{ij}} + \hat{\mathrm{x}}_{\mathrm{ij}} = \sigma^{\varepsilon}_{\mathrm{ij}} - \zeta_{\mathrm{ij}}$ is the classical thermodynamic stress.

If the expression $Z_T = \frac{T}{2\rho_0 k_T} \frac{q_{h_i}}{T} \frac{q_{h_i}}{T}$ is adopted for the component of the force potential that considers the thermal dissipation, the classical Fourier law of heat transport is obtained after the state equation $-T_{,i} = \rho_0 \frac{\partial Z_T}{\partial \frac{q_{h_i}}{T}} \rightarrow q_{h_{i,i}} = -k_T T_{,ii}$. Where the material constant k_T is the thermal conductivity of the porous continuum often evaluated as the geometric mean weighed by

volumetric fractions $k_T = k_s^{1-\phi} + k_f^{\phi}$. Then after the complementary state equations of the porous continuum (Tab.A2) and under assumptions of stationarity and homogeneity conditions Eq.A18 simplifies to,

$$\frac{\partial T}{\partial t} = \frac{1}{c_p}\underbrace{\left(\underbrace{m_f T \left.\frac{-\partial\left(\frac{\phi}{m_f}\right)}{\partial T}\right|_{P}}_{L_p}\frac{\partial P}{\partial t} + \underbrace{\rho T \left.\frac{-\partial\left(\frac{\sigma'_{ij}}{\rho}\right)}{\partial T}\right|_{\varepsilon^e_{ij}}}_{\mathbf{L}^{\varepsilon}}\dot{\varepsilon}^e_{ij} - \underbrace{\rho T \left.\frac{-\partial\left(\frac{\zeta_{ij}}{\rho}\right)}{\partial T}\right|_{\chi_{ij}}}_{\mathbf{L}^{\chi}}\dot{\chi}_{ij}\right)}_{-L} + \frac{1}{c_p}\underbrace{\left(\tilde{x}_{ij}\dot{\varepsilon}^p_{ij} + \underbrace{\left(\frac{\sigma'_{ij}}{2} - \zeta_{ij}\right)}_{\hat{x}_{ij}}\dot{\chi}_{ij}\right)}_{d_s} + C_{th}T_{,ii} \tag{A25}$$

that represents a detailed expression of the temperature field equation in the porous continuum. In Eq.A25 we can distinguished the mechanical dissipation d_s, the thermal diffusivity C_{th} and the latent energy L. The latent energy is composed of three terms: L_p related the thermal expansion of the fluid, L^{ϵ} related to the thermal expansion of the solid and L^{χ} related to the transformation of the hardening state, (Sec. 2).

If the expression $Z_f = -\frac{\eta_f}{2\rho_0 k} q_{f_i} q_{f_i}$ is adopted for the component of the force potential that considers the dissipation due to the fluid flow, the classical Darcy's law of fluid transport is obtained after the state equation $\left(\rho_f\left(g_i - a_{f_i}\right) - P_{,i}\right) = \rho_0 \frac{\partial Z_f}{\partial q_{f_i}}\Big|_{\dot{\varepsilon}^p_{ij}, \dot{\chi}_{ij}, \frac{q_{h_i}}{T}} \rightarrow q_{f_i} = \frac{k}{\eta_f}\left(\rho_f\left(g_i - a_{f_i}\right) - P_{,i}\right)$. Where the isotropic material constant k is the intrinsic permeability of the porous continuum and η_f is the dynamic viscosity of the fluid modeled by the exponential law $\eta_f = \eta_0 exp\left(-\chi_T T\right)$ (NIST, https://webbook.nist.gov/). Combining the isotropic Darcy's law and the continuity equation for the porous continuum Eq.A3 the field equation that describe the rate of change of fluid pressure P in the porous continuum is obtained,

$$\frac{\partial P}{\partial t} = C_{hy} P_{,ii} + \Lambda \frac{\partial T}{\partial t} - \frac{1}{\beta^*}\dot{\varepsilon}_{ii} \tag{A26}$$

where $C_{hy} = \frac{k}{\beta^* \eta_f}$ is the hydraulic conductivity, β^* is the compressibility of the porous continuum and Λ is the thermal pressurization coefficient of the porous continuum (see Monfared et al.[2], Rattez et al.[6]).

B THERMO-MECHANICAL MODEL

The layout of the Gibbs energy density function is not arbitrary. The intermediate energy term L (Eq.9), between the elastic energy g_e and the blocked energy V, defines the type of kinematic hardening as well as the split of total strain usually considered as the sum of an elastic component and a plastic one. A particular layout of the Gibbs energy function to modelized a kinematic hardening was proposed in Collins[34]. However, a generalization is needed in the case that the history of the material can not be described by the plastic strains only and other internal variables must be considered. Such is the case in a thermo-mechanical scenario with thermal hardening where the internal variables for an isotropic thermo-mechanical problem are ε^p_v and χ. Differentiating the volumetric strain $\varepsilon_v = \left.\frac{\partial g_s}{\partial p'}\right|_{T,\varepsilon^p_v,\chi}$ with respect to time leads to,

$$\dot{\varepsilon}_v = \left.\frac{\partial^2 g_s}{\partial p'^2}\right|_{T,\varepsilon^p_v,\chi}\dot{p'} + \left.\frac{\partial^2 g_s}{\partial T \partial p'}\right|_{p',\varepsilon^p_v,\chi}\dot{T} + \left.\frac{\partial^2 g_s}{\partial \varepsilon^p_v \partial p'}\right|_{p',T,\chi}\dot{\varepsilon}^p_v + \left.\frac{\partial^2 g_s}{\partial \chi \partial p'}\right|_{p',\mathrm{T},\varepsilon^p_v}\dot{\chi} \tag{B27}$$

where the first term corresponds to the compliance bulk modulus (for Cam-clay $\frac{\kappa}{p'}$) which is independent of T, ε^p_v and χ; and the second term is the thermal expansion of the porous solid (3α) which is also independent of the rest of variables p', ε^p_v and χ. If it is assumed that two moduli $\left.\frac{\partial^2 g_s}{\partial \varepsilon^p_v \partial p'}\right|_{p',\mathrm{T},\chi}$ and $\left.\frac{\partial^2 g_s}{\partial \chi \partial p'}\right|_{p',T,\varepsilon^p_v}$ are not coupled each term can be integrated separately along a stress path $p_0 - p'$ and the Gibbs energy density can take the general form,

$$g_s\left(p', T, \varepsilon^p_v, \chi\right) = g_e\left(p', T\right) + \underbrace{p' \cdot G_1\left(\varepsilon^p_v\right) + p' \cdot G_2\left(\chi\right)}_{L} + V\left(\chi, T\right) \tag{B28}$$

If the functions G_1 and G_2 are assumed such that $G_1\left(\varepsilon_v^p\right) = \frac{1}{2}\varepsilon_v^p$ and $G_2\left(\chi\right) = \frac{1}{2}\chi$, Eq.B28 can be re-written as,

$$g_s\left(p', \mathrm{T}, \varepsilon_v^p, \chi\right) = g_e\left(p', T\right) + \frac{p'}{2}\left(\varepsilon_v^p + \chi\right) + V\left(\chi, T\right) \tag{B29}$$

Therefore the volumetric strain will be

$$\varepsilon_v = \left.\frac{\partial g_s}{\partial p'}\right|_{T,\varepsilon_v^p,\chi} = \underbrace{\left.\frac{\partial g_e}{\partial p'}\right|_{T,\varepsilon_v^p,\chi}}_{\varepsilon_v^e} + \frac{1}{2}\left(\varepsilon_v^p + \chi\right) \tag{B30}$$

That is the classical split, one elastic component and one plastic component, for the particular case $\varepsilon_v^p = \chi$. Moreover, the mean effective thermodynamic stress p_x is obtained as the sum of $\tilde{p}_x = \left.\frac{\partial g_s}{\partial \varepsilon_v^p}\right|_{p',T,\chi} = \frac{p'}{2}$ and $\hat{p}_x = \left.\frac{\partial g_s}{\partial \chi}\right|_{p',T,\varepsilon_v^p} = \frac{p'}{2} - p_\zeta$ such that $p_x = p' - p_\zeta$ which represents a thermo-mechanical kinematic hardening of the Ziegler type.

The Gibbs energy density function g_s can be partially inverted with respect to the stress invariants, leading to the Helmholtz energy density of the porous solid $f_s = g_s - \left(p'\varepsilon_v + q\varepsilon_s\right)$. It has the explicit form,

$$f_s = \kappa_\epsilon \frac{p_o}{\rho_0}\exp\left(\frac{\tilde{\varepsilon}_v}{\kappa_\epsilon}\right) + \frac{3G}{2\rho_0}\left(\varepsilon_s - \varepsilon_s^p\right)^2 - \left(T - T_0\right)\left(s_{s0} + \left(c_s^e + c_s^b\right)\frac{T - T_0}{2T_0}\right) - \frac{v_\epsilon p_{c0}}{2\rho_0}\exp\left(\frac{\chi - 3\alpha_p\tau_c}{v_\epsilon}\right) \tag{B31}$$

where $\tilde{\varepsilon}_v = \varepsilon_v - 3\alpha\tau\text{-}\frac{\varepsilon_v^p + \chi}{2}$. Thus the rate form of the dependent variables $\left(p', q, s_s\right)$ conjugated to $\left(\varepsilon_v, \varepsilon_s, T\right)$ are given by the expressions,

$$\begin{aligned}
\dot{p}' &= \frac{p_o}{\kappa_\epsilon}\exp\left(\frac{\tilde{\varepsilon}_v}{\kappa_\epsilon}\right)\dot{\varepsilon}_v - \frac{3\alpha p'}{\kappa_\epsilon}\dot{T} + \frac{p'}{\kappa_\epsilon}\frac{\left(\dot{\varepsilon}_v^p + \dot{\chi}\right)}{2} \\
\dot{q} &= 3G\left(\dot{\varepsilon}_s - \dot{\varepsilon}_s^p\right) \\
\rho_0\dot{s}_s &= \frac{3\alpha p'}{\kappa_\epsilon}\dot{\varepsilon}_v + \left(\rho_0\frac{c_s^e + c_s^b}{T_0} + 3\alpha_p\frac{L_\chi}{T}\right)\dot{T} + \frac{L_\chi}{T}\dot{\chi}
\end{aligned} \tag{B32}$$

C GENERALIZED PLASTIC MODULUS

Unlike what is proposed in the classical formulation of bounding plasticity, the thermodynamic formulation of this framework naturally introduces a mapping rule of the plastic modulus variation in the domain between the yield and the bounding surfaces. Since the yield surface is implicitly expressed as $f^y = f^y\left(\underbrace{p' - p_\zeta}_{p_x}, \underbrace{q - q_\zeta}_{q_x}, \varepsilon_v^p, \varepsilon_s^p\right)$ the consistency condition at yielding state is,

$$\begin{aligned}
0 = df^y &= \frac{\partial f^y}{\partial p_x}dp_x + \frac{\partial f^y}{\partial q_x}dq_x + \frac{\partial f^y}{\partial \varepsilon_v^p}d\varepsilon_v^p + \frac{\partial f^y}{\partial \varepsilon_s^p}d\varepsilon_s^p \\
&= \frac{\partial f^y}{\partial p_x}dp_x + \frac{\partial f^y}{\partial q_x}dq_x - \frac{\partial f^y}{\partial p_x}\frac{\partial^2\tilde{V}}{\partial\left(\varepsilon_v^p\right)^2}d\varepsilon_v^p - \frac{\partial f^y}{\partial q_x}\frac{\partial^2\tilde{V}}{\partial\left(\varepsilon_s^p\right)^2}d\varepsilon_s^p
\end{aligned} \tag{C33}$$

By using the mapping rule of scaling Eq.19 $\left(p_x = \frac{1}{\delta}\bar{p}_x - \frac{\beta_0 V}{\delta^2}\frac{\partial\delta}{\partial\varepsilon_v^p}\right)$ the incremental form dp_x can be written as,

$$dp_x = \left\{dp' - \tfrac{1}{\delta}d\bar{p}_\zeta\right\} + \underbrace{\left(\frac{1}{\delta^2}\frac{2\beta_0 V}{\delta}\frac{\partial\delta}{\partial\varepsilon_v^p}\frac{\partial\delta}{\partial\varepsilon_v^p} - \frac{\beta_0 V}{\delta^2}\frac{\partial^2\delta}{\partial\left(\varepsilon_v^p\right)^2}\right)}_{a_{p1}} d\varepsilon_v^p + \underbrace{\left(\frac{1}{\delta^2}\beta_0\frac{\partial V}{\partial\varepsilon_v^p}\frac{\partial\delta}{\partial\varepsilon_s^p} + \frac{1}{\delta^2}\frac{2\beta_0 V}{\delta}\frac{\partial\delta}{\partial\varepsilon_v^p}\frac{\partial\delta}{\partial\varepsilon_s^p} - \frac{\beta_0 V}{\delta^2}\frac{\partial^2\delta}{\partial\varepsilon_s^p\partial\varepsilon_v^p}\right)}_{a_{p2}} d\varepsilon_s^p \tag{C34}$$

where the expression $d\bar{p} = \delta\cdot dp' + \left(\frac{\partial\delta}{\partial\varepsilon_v^p}d\varepsilon_v^p + \frac{\partial\delta}{\partial\varepsilon_s^p}d\varepsilon_s^p\right)p'$ has been used. In the same way, by using the mapping rule of scaling $\left(q_x = \frac{1}{\delta}\bar{q}_x - \frac{\beta_0 V}{\delta^2}\frac{\partial\delta}{\partial\varepsilon_s^p}\right)$ the incremental form dq_x can be written as,

$$dq_x = dq + \underbrace{\left(\frac{1}{\delta^2}\frac{2\beta_0 V}{\delta}\frac{\partial\delta}{\partial\varepsilon_s^p}\frac{\partial\delta}{\partial\varepsilon_v^p} - \frac{\beta_0 V}{\delta^2}\frac{\partial^2\delta}{\partial\varepsilon_v^p\partial\varepsilon_s^p}\right)}_{a_{q1}} d\varepsilon_v^p + \underbrace{\left(-\frac{1}{\delta^2}\beta_0\frac{\partial V}{\partial\varepsilon_v^p}\frac{\partial\delta}{\partial\varepsilon_s^p} + \frac{1}{\delta^2}\frac{2\beta_0 V}{\delta}\frac{\partial\delta}{\partial\varepsilon_s^p}\frac{\partial\delta}{\partial\varepsilon_s^p} - \frac{\beta_0 V}{\delta^2}\frac{\partial^2\delta}{\partial\left(\varepsilon_s^p\right)^2}\right)}_{a_{q2}} d\varepsilon_s^p \tag{C35}$$

where the expression $d\bar{q} = \delta\cdot dq + \left(\frac{\partial\delta}{\partial\varepsilon_v^p}d\varepsilon_v^p + \frac{\partial\delta}{\partial\varepsilon_s^p}d\varepsilon_s^p\right)q$ has been used. The last two terms in the right hand side of Eq. C33 can be developed in order to highlight the function's derivatives of the radial distance (δ), leading to,

$$dp_\zeta = \frac{\beta_0}{\delta}\frac{\partial^2 V}{\partial\left(\varepsilon_v^p\right)^2}d\varepsilon_v^p + \underbrace{\left(\frac{\partial\delta}{\partial\varepsilon_v^p}\frac{\partial^2\tilde{V}}{\partial\delta\partial\varepsilon_v^p} + \frac{\partial\delta}{\partial\varepsilon_v^p}\left(\frac{\partial^2\tilde{V}}{\partial\delta\partial\varepsilon_v^p} + \frac{\partial\delta}{\partial\varepsilon_v^p}\frac{\partial^2\tilde{V}}{\partial\delta^2}\right) + \frac{\partial\tilde{V}}{\partial\delta}\frac{\partial^2\delta}{\partial\left(\varepsilon_v^p\right)^2}\right)}_{\tilde{a}_v} d\varepsilon_v^p + \underbrace{\left(\frac{\partial\delta}{\partial\varepsilon_s^p}\frac{\partial^2\tilde{V}}{\partial\delta\partial\varepsilon_v^p} + \frac{\partial\tilde{V}}{\partial\delta}\frac{\partial^2\delta}{\partial\varepsilon_v^p\partial\varepsilon_s^p} + \frac{\partial\delta}{\partial\varepsilon_s^p}\frac{\partial\delta}{\partial\varepsilon_v^p}\frac{\partial^2\tilde{V}}{\partial\delta^2}\right)}_{\tilde{a}_s} d\varepsilon_s^p \tag{C36}$$

On the other side, the rate of the mean back stress at bounding $\bar{p}_\zeta$ is,

$$d\bar{p}_\zeta = \beta_0\frac{\partial^2 V}{\partial\left(\varepsilon_v^p\right)^2}d\varepsilon_v^p \tag{C37}$$

Combining Eq.C33 to Eq.C37 the following expressions for the plastic strain increments are obtained,

$$d\varepsilon_v^p = \frac{d_f\frac{\partial f^y}{\partial p_x}}{H_p + H_\delta}\ ;\ d\varepsilon_s^p = \frac{d_f\frac{\partial f^y}{\partial q_x}}{H_p + H_\delta} \tag{C38}$$

where $d_f = \frac{\partial f^y}{\partial p_x} dp + \frac{\partial f^y}{\partial q_x} dq$, and the plastic modulus of pure yielding H_p and the bounding modulus H_δ are given by,

$$H_p = \frac{\partial f^y}{\partial p_x}\left(\frac{2\beta_0}{\delta}\frac{\partial^2 V}{\partial\left(\varepsilon_v^p\right)^2}\right)\frac{\partial f^y}{\partial p_x}\underbrace{+\frac{\partial f^y}{\partial p_x}\tilde{a}_v\frac{\partial f^y}{\partial p_x}+\frac{\partial f^y}{\partial q_x}\tilde{a}_s\frac{\partial f^y}{\partial q_x}}_{\text{extension due to enhanced block}}$$
$$H_\delta = -\left\{\left(\frac{\partial f^y}{\partial p_x}a_{p1}+\frac{\partial f^y}{\partial q_x}a_{q1}\right)\frac{\partial f^y}{\partial p_x}+\left(\frac{\partial f^y}{\partial p_x}a_{p2}+\frac{\partial f^y}{\partial q_x}a_{q2}\right)\frac{\partial f^y}{\partial q_x}\right\} \tag{C39}$$

It is noticed the dependency of H_δ on the radial distance.